Mathematics

http://www.aimspress.com/journal/Math

AIMS Mathematics, 11(4): 11840–11881.
DOI: 10.3934/math.2026487
Received: 23 January 2026
Revised: 20 March 2026
Accepted: 30 March 2026
Published: 28 April 2026

Research article

A new Weibull reliability modeling under adaptive progressive censoring and its applications in engineering and physical sciences

Ahmed Elshahhat[1,*], Osama E. Abo-Kasem[2] and Heba S. Mohammed[3]

[1] Faculty of Technology and Development, Zagazig University, Zagazig 44519, Egypt
[2] Department of Statistics, Faculty of Commerce, Zagazig University, Zagazig 44519, Egypt
[3] Department of Mathematical Sciences, College of Science, Princess Nourah bint Abdulrahman University, P.O. Box 84428, Riyadh 11671, Saudi Arabia

* **Correspondence:** Email: aelshahhat@ftd.zu.edu.eg; Tel: +201225939600.

Abstract: This study developed several inferential procedures for a modified and highly flexible extension of the classical Weibull distribution, termed the very flexible Weibull (VFW) distribution. Statistical inference was conducted under an adaptive progressive censoring scheme, which enhances dynamic control over the test duration and sample utilization. Both likelihood-based and Bayesian estimation methods were established for the model parameters and associated reliability measures. Nonlinear likelihood equations were derived and solved numerically using the Newton–Raphson iterative method, and asymptotic confidence intervals were constructed under normal and log-normal approximations. Within the Bayesian framework, independent gamma priors were assumed, and posterior inference was carried out using Markov chain Monte Carlo simulation based on the Metropolis–Hastings algorithm to obtain posterior summaries and two types of credible intervals. A numerical assessment was conducted to evaluate the statistical performance of the proposed estimators under various adaptive censoring configurations and prior specifications. The simulation results demonstrated that Bayesian estimators, particularly under informative priors, provide superior bias reduction, improved coverage probabilities, and more stable interval estimates than their frequentist counterparts. To illustrate the practical applicability of the proposed methodology, two real engineering datasets were analyzed. The data analysis confirmed the excellent fitting capability of the VFW distribution for modeling complex lifetime behaviors. From an engineering standpoint, the data-driven outcomes underscore the VFW distribution as a flexible and dependable lifetime model that facilitates precise reliability evaluation and decision-making in actual industrial systems.

Keywords: Weibull; Markov chain; optimum; reliability; censoring; carbon fibers; river floods; nonlinear optimization
Mathematics Subject Classification: 62F10, 62F15, 62N01, 62N02, 62N05

1. Introduction

The Weibull model has long been an important issue in reliability and lifetime data analysis. This interest stems from the fact that many engineering and industrial applications require statistical models capable of describing complex, non-monotonic failure behaviors. The standard Weibull model, despite its popularity, is restricted to monotonic failure rate (FR) forms, either increasing or decreasing, while real-life systems often exhibit more intricate patterns such as unimodal, bathtub-shaped, or modified bathtub-shaped FRs. This limitation has motivated numerous attempts to generalize the Weibull model to capture a wider range of reliability characteristics within a single analytical framework. Thus, different modifications and extensions were introduced, e.g., additive Weibull, flexible Weibull, and modified Weibull, which were specifically designed to produce different FR shapes; see, for example, Almalki and Yuan [1].

In statistical modeling and reliability analysis, the development of flexible extensions of the traditional Weibull distribution has long been a central topic. Despite the Weibull model being one of the most extensively utilized lifetime distributions, it is inherently limited to representing monotonic failure rate behaviors, either strictly increasing or strictly decreasing. However, many real-world systems display more complex patterns, such as unimodal, bathtub-shaped, or modified bathtub-shaped FRs. To address this limitation, the very flexible Weibull (VFW) distribution, a two-parameter generalization of the classical Weibull law, was originally proposed by Ahmad and Hussain [2].

Recently, in the presence of progressive Type-II censoring (T2-PC), Brito et al. [3] evaluated the VFW parameters. This distribution is created by formulating its cumulative FR as a mixture of logarithmic versions of two distinct cumulative FRs, allowing for greater flexibility in modeling lifetime data. This model is capable of capturing a wide range of hazard rate shapes, including monotone increasing, unimodal (increase → decrease), and multi-turning-point (increase → decrease → increase) shapes, making it particularly well-suited for modeling complex degradation and fatigue processes commonly encountered in engineering, reliability, and physical sciences. In the next section, a brief formulation of the VFW distribution will be explored. Let Y be a non-negative random variable following the VFW($\boldsymbol{\theta}$) distribution, where $\boldsymbol{\theta} = (\gamma, \delta)^\top$ and $\gamma > 0$ and $\delta > 0$ represent the shape and scale parameters, respectively. Then, its probability density function (PDF, $g(\cdot)$) and cumulative distribution function (CDF, $G(\cdot)$) are given as

$$g(y; \boldsymbol{\theta}) = (\gamma\delta y^{\gamma-1} + y^{-2}) \exp(\delta y^\gamma - y^{-1}) \exp(-\exp(\delta y^\gamma - y^{-1})), \quad y > 0, \tag{1.1}$$

and

$$G(y; \boldsymbol{\theta}) = 1 - \exp(-\exp(\delta y^\gamma - y^{-1})), \tag{1.2}$$

respectively.

The VFW distribution's reliability function (RF), $R(\cdot)$, and failure rate function (HRF), $h(\cdot)$, are expressed as

$$R(t; \boldsymbol{\theta}) = \exp(-\exp(\delta t^\gamma - t^{-1})),\ t > 0, \tag{1.3}$$

and

$$h(t; \boldsymbol{\theta}) = (\gamma\delta t^{\gamma-1} + t^{-2}) \exp(\delta t^\gamma - t^{-1}), \tag{1.4}$$

respectively.

Notably, when $\gamma = 1$, the VFW model reduces to a double exponential (Gumbel-type) distribution, and for certain parameter limits, it encompasses other well-known lifetime models such as the exponentiated Weibull (by Mudholkar and Srivastava [4]) and flexible Weibull (by Bebbington et al. [5]). Figure 1(a) reveals that the density (1.1) can be decreasing, unimodal (right- or left-skewed), or bimodal, based on parameter settings. In contrast, the corresponding HRF shapes in Figure 1(b), for $\gamma > 0$, exhibit the following possible shapes. If $\delta < 0$, the HRF is unimodal (increase → decrease). If $\delta = 0$, the HRF is also unimodal. If $\delta > 0$, the HRF is either strictly monotone increasing or follows an increase → decrease → increase pattern. For additional details on the VFW failure rate patterns, see Elshahhat and Seyam [6].

It is worth noting that the VFW distribution can be viewed within the broad class of transformed lifetime models commonly used in survival and reliability analysis. In particular, its RF can be expressed in the complementary log-log form $R(t;\boldsymbol{\theta}) = \exp(-\exp(\eta(t)))$, where $\eta(t) = \delta t^{\gamma} - t^{-1}$ is a predictor term. From this perspective, the VFW formulation may be interpreted as a parametric specification of the cumulative HRF that extends a Weibull-type component through the inclusion of an additional inverse-time term; see Kalbfleisch and Prentice [7]. Consequently, the model may be regarded as one member of the broader family of Weibull-based or transformed lifetime distributions that achieve flexible hazard shapes through suitable transformations of a baseline model. To cover a wide range of survival distribution families that go beyond the Weibull lifespan model, one can easily refer to Lawless [8].

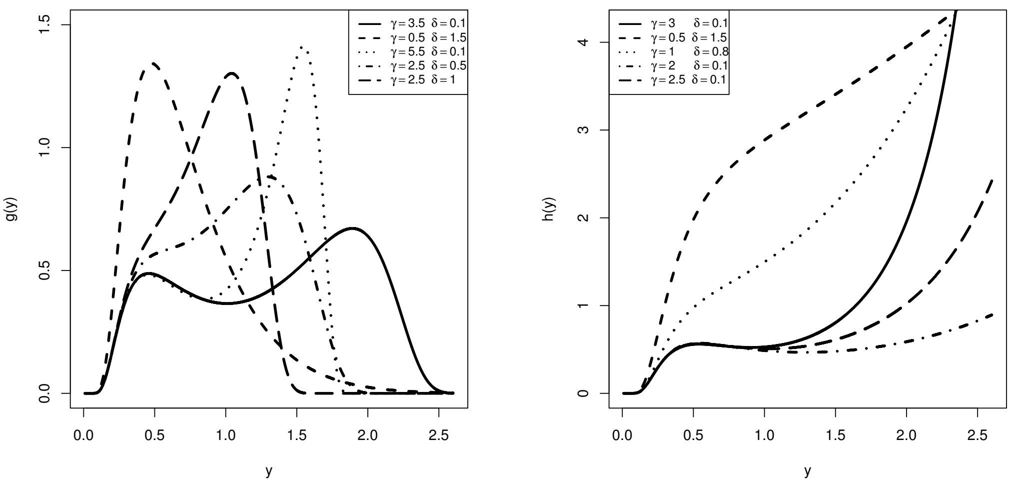

(a) PDF (b) HRF

Figure 1. The density and hazard rate shapes of the VFW distribution.

Although the VFW distribution has proven particularly useful for analyzing lifespan and reliability data characterized by wear-out phenomena or early-life failures, few studies in the literature have focused on it, except Brito et al. [3], who investigated several estimation methods for VFW parameters via the T2-PC strategy and showed that the distribution provides excellent fit performance compared to several existing competing alternatives.

Progressive censoring is a life-testing design commonly used in reliability experiments in which a predetermined number of surviving test units may be intentionally removed from the experiment at different stages during the testing process before the termination time point. Specifically, after each observed failure time, a fixed or pre-specified number of the remaining units that have not yet failed are randomly withdrawn from the experiment according to a censoring scheme. One of the best modifications of T2-PC strategies, called an adaptive T2-PC (T2A-PC), by Ng et al. [9], aimed at improving the efficiency of statistical inference. In this design, the failure limit k (out of n) is predetermined, and the test is allowed to continue beyond a specified time threshold T under a progressive censoring plan $\mathbf{S} = (S_1, S_2, \ldots, S_k)$, which may be corrected adaptively during the examination. The censoring mechanism follows the same general structure as the T2-PC, but with a different stopping rule. Specifically, if the k^{th} failure occurs before T (i.e., $Y_{k:k:n} < T$), the experiment terminates at $Y_{k:k:n}$. Otherwise, if $Y_{d:k:n} < T < Y_{d+1:k:n}$ for some $d+1 < k$, the experimenter ceases further removals by setting $S_{d+1} = S_{d+2} = \cdots = S_{k-1} = 0$ and $S_k = n - k - \sum_{j=1}^{d} S_j$. This adaptive rule ensures that the desired number of failures k is eventually observed while maintaining control over the duration and efficiency of the experiment.

Let $\{\mathbf{Y}, \mathbf{S}\} = \{(y_{1:k:n}, S_1), \ldots, (y_{d:k:n}, S_d), T, (y_{d+1:k:n}, 0), \ldots, (y_{k-1:k:n}, 0), (y_{k:k:n}, S_k)\}$ be a T2A-PC sample; then, the likelihood function (LF) of the collected T2A-PC data is

$$\mathcal{L}(\boldsymbol{\theta}|\mathbf{y}) = \Omega \prod_{i=1}^{k} g(y_{i:k:n}) \prod_{i=1}^{d} [1 - G(y_{i:k:n})]^{S_i} [1 - G(y_{k:k:n})]^{S_k}, \tag{1.5}$$

where Ω denotes the parameter-free term. For clarification, a full list of abbreviations and symbol descriptions was provided in Appendix 2.

Numerous works by various a variety of authors have evaluated the effectiveness of the proposed strategy under various lifetime models. For example, Liu and Gui [10] (for the Rayleigh model), Elshahhat and Nassar [11] (for the Hjorth model), Chen and Gui [12] (for the bathtub-shaped HRF distribution), Kazempoor et al. [13] (for the Weibull distribution), Lv et al. [14] (for the Gompertz distribution), Dutta et al. [15] (for the logistic exponential distribution), Kohansal et al. [16] (for the Kumaraswamy generalized distribution), and Sharma and Kumar [17] (for the Lomax distribution), among others.

The growing need for robust and flexible lifetime models that can accurately describe complex and non-monotonic failure behaviors in engineering and physical systems provides the central motivation for this study. Traditional Weibull-based models, though widely used, are limited to monotonic hazard rate patterns and thus often fail to capture real-world lifespan data exhibiting diverse FRs, wear-out phenomena, or non-monotonic hazard structures. To overcome these challenges, this work develops a comprehensive investigation plan for the VFW model from T2A-PC as an advanced design that enhances data efficiency, inference precision, and experimental control.

In contrast, in reliability and life-testing experiments, practical constraints such as limited experimental time, high testing costs, and equipment availability often prevent researchers from observing complete lifetime data. As a result, T2A-PC has attracted increasing attention because it provides greater flexibility in balancing test duration and the number of observed failures. Motivated by these practical considerations, both classical and Bayesian estimation approaches are investigated to assess their performance in estimating the model parameters and associated reliability characteristics when incomplete data arise from adaptive progressive censoring.

Thus, the integration of the VFW model using T2A-PC enables superior adaptability in modeling real-world reliability data while maintaining analytical tractability, thus offering a unified, efficient, and practical tool for reliability analysis under complex censoring structures. As a limitation, the estimation procedures proposed are evaluated primarily through classical and Bayesian approaches under T2A-PC data, while alternative inferential frameworks or more complex censoring mechanisms could also be explored. The novel contributions of this study are sixfold:

- An analysis of the VFW model based on T2A-PC is introduced, offering a superior and flexible platform for analyzing adaptive censoring data.
- Several analytical expressions for the joint likelihood and asymptotic properties of the VFW parameters are derived, allowing efficient frequentist estimation under the proposed censoring.
- Model parameters γ and δ, RF, and HRF are estimated using both maximum likelihood estimation (MLE) and Bayesian inferential frameworks. A tailored Markov chain Monte Carlo (MCMC) approach is used to provide Bayesian results and credible ranges for the proposed model's complex posterior structure.
- Different interval estimation methods, including asymptotic normal, log-transformed, and highest posterior density (HPD) credible intervals, are systematically evaluated for their coverage accuracy and robustness.
- Extensive Monte Carlo simulations based on four metrics of estimation precision demonstrate the superiority, flexibility, and practical relevance of the proposed methods in modeling censored reliability data.
- Through two real-life engineering and physical science applications, the proposed VFW model demonstrates clear superiority over twelve existing lifetime models in the literature, achieving the best overall fit and predictive performance based on standard information criteria and graphical diagnostics, thereby confirming its exceptional flexibility and reliability modeling power.

The rest of the work is arranged as follows: Sections 2 and 3 present the frequentist and Bayesian procedures, respectively. Monte Carlo simulations are implemented in Section 4. Real-data applications are analyzed in Section 5. Section 6 provides a concise discussion on optimal censoring metrics. Finally, concluding observations and future research goals are highlighted in Section 7.

2. Likelihood inference

This section uses T2A-PC data to derive MLEs for the coefficients (γ, δ) and reliability characteristics $(R(t), h(t)$ of the VFW distribution. In addition, two-sided $(1-\varphi)100\%$ ACIs for these values are created.

2.1. Likelihood estimators

Suppose $Y_i \cong Y_{i:k:n}$, $i = 1, 2, \ldots, d$ $(1 \leqslant d \leqslant n)$, is a T2A-PC sample acquired from the VFW($\boldsymbol{\theta}$) having a fixed $\mathbf{S}$. Substituting (1.1) and (1.2) into (1.5), the joint LF of γ and δ can be written as

$$\mathcal{L}(\theta|\,\mathbf{y}) \propto \exp\left(-\left[\sum_{i=1}^{k}(\xi_i - \log(\xi_i)) + \sum_{i=1}^{d} S_i\xi_i + S^*\xi_k\right]\right)\prod_{i=1}^{k}\zeta_i, \tag{2.1}$$

where $\xi_i = \xi(y_i; \gamma, \delta) = e^{\delta y_i^{\gamma} - y_i^{-1}}$, $i = 1, 2, ..., k$, and $\zeta_i = \zeta(y_i; \gamma, \delta) = \gamma\delta y_i^{\gamma-1} + y_i^{-2}$.

The log-LF ($\mathcal{L}^{\star}(\cdot) \propto \log \mathcal{L}(\cdot)$), from (2.1), is

$$\mathcal{L}^{\star}(\theta|\mathbf{y}) \propto \sum_{i=1}^{k}\left(\delta y_i^{\gamma} - \xi_i\right) + \sum_{i=1}^{k}\log(\zeta_i) - \sum_{i=1}^{d} S_i\xi_i - S^*\xi_k. \tag{2.2}$$

By differentiating (2.2) with respect to γ and δ, the associated expressions are:

$$\delta\sum_{i=1}^{k} y_i^{\gamma}\log(y_i) - \sum_{i=1}^{k}\xi_i^{\circ} - \sum_{i=1}^{d} S_i\xi_i^{\circ} - S^*\xi_k^{\circ} + \sum_{i=1}^{k}\zeta_i^{\circ}\zeta_i^{-1}\Bigg|_{(\hat{\gamma},\hat{\delta})} = 0 \tag{2.3}$$

and

$$\sum_{i=1}^{k} y_i^{\gamma} - \sum_{i=1}^{k}\xi_i^{\bullet} - \sum_{i=1}^{d} S_i\xi_i^{\bullet} - S^*\xi_k^{\bullet} + \sum_{i=1}^{k}\zeta_i^{\bullet}\zeta_i^{-1}\Bigg|_{(\hat{\gamma},\hat{\delta})} = 0, \tag{2.4}$$

respectively, where

$$\zeta_i^{\circ} = \delta y_i^{\gamma-1}(1+\gamma\log(y_i)),\ \zeta_i^{\bullet} = \gamma y_i^{\gamma-1},\ \xi_i^{\circ} = \delta y_i^{\gamma}\log(y_i)\,\xi_i, \text{ and } \xi_i^{\bullet} = y_i^{\gamma}\xi_i, \text{ for } i = 1,2,...,k.$$

Equations (2.3) and (2.4) show that solving a system of nonlinear equations yields the MLEs $\hat{\gamma}$ and $\hat{\delta}$. As a result, a suitable iterative process, such as the Newton-Raphson method, is used to get these estimations. As a recommendation, the `maxLik` R-package, proposed by Henningsen and Toomet [18], is utilized. Subsequently, by substituting γ and δ with their corresponding MLEs $\hat{\gamma}$ and $\hat{\delta}$, the MLEs $\hat{R}(t)$ and $\hat{h}(t)$ are developed as:

$$\hat{R}(t;\boldsymbol{\theta}) = \exp(-\exp(\hat{\delta}t^{\hat{\gamma}} - t^{-1}))$$

and

$$\hat{h}(t;\boldsymbol{\theta}) = (\hat{\gamma}\hat{\delta}t^{\hat{\gamma}-1} + t^{-2})\exp(\hat{\delta}t^{\hat{\gamma}} - t^{-1}),$$

respectively.

Corollary 1. The results by Brito et al. [3] can be easily obtained by setting $T \to \infty$ in (2.2).

2.2. Asymptotic interval estimators

To construct the $100(1-\varphi)\%$ ACI estimators of γ, δ, $R(t)$, and $h(t)$, the asymptotic properties of their MLEs are employed based on the large sample size. The asymptotic distribution of $\boldsymbol{\theta}$ follows a bivariate normal distribution with mean $\boldsymbol{\theta}$ and a variance–covariance, $\mathbf{F}^{-1}(\cdot)$, matrix (VCM). In practice, the Fisher, $\mathbf{F}(\cdot)$, information matrix (FIM) is approximated by its observed counterpart at $\boldsymbol{\theta} = \hat{\boldsymbol{\theta}}$. As a sequence, the estimated VCM of $\hat{\gamma}$ and $\hat{\delta}$ must be obtained first as

$$\mathbf{F}^{-1}(\hat{\boldsymbol{\theta}}) \cong \begin{bmatrix} -\mathcal{L}_{11}^{\star} & -\mathcal{L}_{12}^{\star} \\ -\mathcal{L}_{21}^{\star} & -\mathcal{L}_{22}^{\star} \end{bmatrix}_{\boldsymbol{\theta}=\hat{\boldsymbol{\theta}}}^{-1} = \begin{bmatrix} \hat{\varepsilon}_{11} & \hat{\varepsilon}_{12} \\ \hat{\varepsilon}_{21} & \hat{\varepsilon}_{22} \end{bmatrix}, \tag{2.5}$$

where $\mathcal{L}_{ij}^{\star}$ (for $i, j = 1, 2$) are given by

$$\mathcal{L}_{11}^{\star} = \delta\sum_{i=1}^{k} y_i^{\gamma}\log^2(y_i) - \sum_{i=1}^{k}\xi_i^{\circ\circ} - \sum_{i=1}^{d} S_i\xi_i^{\circ\circ} - S^*\xi_k^{\circ\circ} + \sum_{i=1}^{k}\left[\zeta_i\zeta_i^{\circ\circ} - (\zeta_i^{\circ})^2\right]\zeta_i^{-2}, \tag{2.6}$$

$$\mathcal{L}^{\star}_{22} = -\sum_{i=1}^{k} \xi_i^{\bullet\bullet} - \sum_{i=1}^{d} S_i \xi_i^{\bullet\bullet} - S^* \xi_k^{\bullet\bullet} + \sum_{i=1}^{k} \left[\zeta_i \zeta_i^{\bullet\bullet} - (\zeta_i^{\bullet})^2 \right] \zeta_i^{-2}, \tag{2.7}$$

and

$$\mathcal{L}^{\star}_{12} = \sum_{i=1}^{k} y_i^{\gamma} \log^2(y_i) - \sum_{i=1}^{k} \xi_i^{\circ\bullet} - \sum_{i=1}^{d} S_i \xi_i^{\circ\bullet} - S^* \xi_k^{\circ\bullet} + \sum_{i=1}^{k} \left[\zeta_i \zeta_i^{\circ\bullet} - \zeta_i^{\circ} \zeta_i^{\bullet} \right] \zeta_i^{-2}, \tag{2.8}$$

where
$\zeta_i^{\circ\circ} = \delta y_i^{\gamma-1} \log(y_i)(2 + \gamma \log(y_i))$, $\zeta_i^{\bullet\bullet} = 0$, $\zeta_i^{\circ\bullet} = y_i^{\gamma-1}(1 + \gamma \log(y_i))$, $\xi_i^{\circ\circ} = \delta y_i^{\gamma}\left(1 + \delta y_i^{\gamma}\right) \log^2(y_i) \xi_i$, $\xi_i^{\bullet\bullet} = y_i^{2\gamma} \xi_i$, and $\xi_i^{\circ\bullet} = y_i^{\gamma}\left(1 + \delta y_i^{\gamma}\right) \log(y_i) \xi_i$ for $i = 1, 2, ..., k$.

The asymptotic properties of the MLEs are derived under the standard regularity conditions commonly assumed in LF-based inference. These conditions include: (i) The true parameter vector lies in the interior of the parameter space; (ii) the log-LF is sufficiently smooth with respect to the model parameters, allowing the existence and continuity of the required first- and second-order derivatives; (iii) the model parameters are identifiable; and (iv) the FIM exists and is positive definite. Under these regularity conditions, the MLEs $\boldsymbol{\theta} = (\hat{\gamma}, \hat{\delta})^{\top}$ of the VFW parameters are consistent and asymptotically normally distributed. Consequently, the asymptotic distribution of the estimator vector $\boldsymbol{\theta}$ can be approximated by a bivariate normal distribution with mean θ and VCM given by the inverse of the FIM. This result provides the theoretical justification for constructing asymptotic confidence intervals based on the normal approximation and the observed FIM.

Thus, based on the normal approximation (NA) of the MLEs $\hat{\gamma}$ and $\hat{\delta}$, the two-sided $100(1-\varphi)\%$ ACIs using the NA-based approach (denoted as ACI-NA) for γ and δ are, respectively, given by

$$\hat{\gamma} \mp z_{0.5\varphi} \sqrt{\hat{\varepsilon}_{11}} \qquad \text{and} \qquad \hat{\delta} \mp z_{0.5\varphi} \sqrt{\hat{\varepsilon}_{22}},$$

where $z_{0.5\varphi}$ is the upper (0.5φ)th probability point of the standard normal distribution.

Additionally, to obtain the ACI-NA estimator of $R(t)$ or $h(t)$, the delta method is used to approximate their variances (see Greene [19]). However, from the VCM (2.5), the approximated variances of $\hat{R}(t)$ and $\hat{h}(t)$, denoted by $\hat{\varepsilon}_{\hat{R}}$ and $\hat{\varepsilon}_{\hat{h}}$, respectively, are given by

$$\hat{\varepsilon}_{\hat{R}} \simeq \mathfrak{I}_R \mathbf{F}^{-1}(\boldsymbol{\theta}) \mathfrak{I}_R^{\top}\Big|_{(\hat{\gamma},\hat{\delta})} \text{ and } \hat{\varepsilon}_{\hat{h}} \simeq \mathfrak{I}_h \mathbf{F}^{-1}(\boldsymbol{\theta}) \mathfrak{I}_h^{\top}\Big|_{(\hat{\gamma},\hat{\delta})},$$

respectively, where $\mathfrak{I}_R = \begin{bmatrix} \mathfrak{I}_R^{\gamma} & \mathfrak{I}_R^{\delta} \end{bmatrix}$ and $\mathfrak{I}_h = \begin{bmatrix} \mathfrak{I}_h^{\gamma} & \mathfrak{I}_h^{\delta} \end{bmatrix}$, such as

$$\mathfrak{I}_R^{\gamma} = -\delta t^{\gamma} e^{-\xi_t} \xi_t \log(t),$$

$$\mathfrak{I}_R^{\delta} = -t^{\gamma} e^{-\xi_t} \xi_t,$$

$$\mathfrak{I}_h^{\gamma} = \delta \left[\left(\gamma t^{\gamma-1} + t^{\gamma} \left(t^{-2} + \gamma \delta t^{\gamma-1} \right) \right) \log(t) + t^{\gamma-1} \right] \xi_t,$$

$$\mathfrak{I}_h^{\delta} = \left(\gamma t^{\gamma-1} + t^{\gamma} \left(t^{-2} + \gamma \delta t^{\gamma-1} \right) \right) \xi_t,$$

where $\xi_t = \xi(t; \gamma, \delta) = e^{\delta t^{\gamma} - t^{-1}}$.

Thus, at a confidence level of $100(1-\varphi)\%$, the ACI-NA estimators of $R(t)$ and $h(t)$ can be obtained, respectively, as

$$\hat{R}(t) \mp z_{0.5\varphi} \sqrt{\hat{\varepsilon}_{\hat{R}}} \quad \text{and} \quad \hat{h}(t) \mp z_{0.5\varphi} \sqrt{\hat{\varepsilon}_{\hat{h}}}.$$

In practice, a major drawback of the conventional ACI-NA method is that it can occasionally produce negative lower limits for parameters that are inherently positive. To address this issue, Meeker and Escobar [20] proposed an alternative approach based on using a logarithmic adjustment to the MLE of γ, δ, $R(t)$, or $h(t)$ before developing the interval. This approach, called the log-transformed approximation ACI (ACI-NL), assures that all interval limits are positive. Furthermore, they observed that although the ACI-NA method may yield much higher coverage probabilities, the ACI-NL approach often provides more reliable interval estimates in finite samples, since the log transformation mitigates the skewness typically present in the sampling distribution of MLEs. However, the $100(1-\varphi)\%$ ACI-NL of γ (as an example) is given by

$$\hat{\gamma}\exp\left(\mp\frac{z_{0.5\varphi}}{\hat{\gamma}}\sqrt{\hat{\varepsilon}_{11}}\right).$$

Now, to sum up, we shall mention the features of the ACI-NA and ACI-NL methods. The ACI-NA intervals are constructed directly from the asymptotic normality of the MLEs using the observed FIM. Although this method is simple and widely used, it may sometimes yield infeasible bounds, particularly when the estimator distribution is skewed or the sample size is small. To mitigate this issue, the ACI-NL method applies a logarithmic transformation to the parameters before constructing the intervals. The limits are then transformed back to the original parameter scale. As a result, the ACI-NL often provides more stable intervals and guarantees positive bounds for parameters that are restricted to be positive.

3. Bayesian inference

In this section, we formulate a Bayesian inference scheme for estimating the parameters γ and δ of the VFW model, along with the associated reliability measure $R(t)$ and hazard function $h(t)$. The corresponding BCI and HPD credible intervals are also constructed. It is assumed that γ and δ are mutually independent at the prior stage, with prior knowledge introduced through suitable prior distributions. Among the available prior specifications, the gamma family is regarded as one of the most versatile and analytically convenient options; see Kundu [21]. Owing to its mathematical simplicity and flexibility, the gamma distribution can effectively represent a wide spectrum of prior information regarding the parameters of interest. In this study, the parameters γ and δ are assumed to be a priori independent and follow gamma distributions; that is, $\gamma \sim \text{Gamma}(a_1, b_1)$ and $\delta \sim \text{Gamma}(a_2, b_2)$, where $a_i, b_i > 0$, $i = 1, 2$, denote the hyperparameters reflecting the experimenter's prior knowledge about the VFW($\boldsymbol{\theta}$) model parameters. Consequently, the joint prior PDF of $\boldsymbol{\theta}$ (say, $\pi(\cdot)$) can be expressed as

$$\pi(\boldsymbol{\theta}) \propto \gamma^{a_1-1}\delta^{a_2-1}e^{-(b_1\gamma+b_2\delta)}, \quad \gamma,\delta > 0,\ a_i, b_i > 0. \tag{3.1}$$

The joint posterior PDF of $\boldsymbol{\theta}$ (say, $\Pi(\cdot)$) is given by

$$\Pi(\boldsymbol{\theta}|\,\mathbf{y}) = \vartheta^{-1}\mathcal{L}(\theta|\,\mathbf{y})\,\pi(\boldsymbol{\theta}), \tag{3.2}$$

where $\vartheta = \int_0^\infty\int_0^\infty \mathcal{L}(\theta|\,\mathbf{y})\,\pi(\boldsymbol{\theta})\,\mathrm{d}\gamma\mathrm{d}\delta$.

Using (2.1) and (3.1), we re-express (3.2) for the VFW parameters γ and δ as

$$\Pi(\boldsymbol{\theta}|\,\mathbf{y}) \propto \gamma^{a_1-1}\delta^{a_2-1}\exp\left(-\left[b_1\gamma + b_2\delta + \sum_{i=1}^{k}(\xi_i - \log(\xi_i)) + \sum_{i=1}^{d} S_i\xi_i + S^*\xi_k\right]\right)\prod_{i=1}^{k}\zeta_i. \tag{3.3}$$

Among the various loss functions used in Bayesian analysis is the squared error loss (SEL), which is the most common symmetric choice. Accordingly, the Bayes estimator (say, $\tilde{\omega}(\cdot)$) of any function of $\boldsymbol{\theta}$, denoted by $\omega(\boldsymbol{\theta})$, is obtained as the posterior mean of $\omega(\boldsymbol{\theta})$. The SEL function, denoted by Ξ, and its corresponding Bayes estimator, $\tilde{\omega}(\boldsymbol{\theta})$, can be expressed, respectively, as

$$\Xi(\omega(\boldsymbol{\theta}), \tilde{\omega}(\boldsymbol{\theta})) = (\tilde{\omega}(\boldsymbol{\theta}) - \omega(\boldsymbol{\theta}))^2$$

and

$$\tilde{\omega}(\boldsymbol{\theta}) = \int_0^{\infty} \int_0^{\infty} \omega(\boldsymbol{\theta}) \mathcal{L}\left(\theta | \, \mathbf{y}\right) \pi\left(\boldsymbol{\theta}\right) \mathrm{d}\gamma \mathrm{d}\delta. \tag{3.4}$$

Evidently, owing to the nonlinear form of (3.3), closed-form expressions for the Bayes estimator using the SEL-based function of γ, δ, $R(t)$, or $h(t)$ are not attainable. An MCMC-based computational approach is adopted to draw samples from the posterior distributions, allowing for the estimation of Bayes estimators and the formation of BCI and HPD estimates. To generate posterior samples using the MCMC procedure, the posteriors of γ and δ are

$$\Pi_{\gamma}\left(\gamma | \delta, \mathbf{y}\right) \propto \gamma^{a_1 - 1} \exp\left(-\left[b_1 \gamma + \sum_{i=1}^{k} \left(\xi_i - \log\left(\xi_i\right)\right) + \sum_{i=1}^{d} S_i \xi_i + S^* \xi_k\right]\right) \prod_{i=1}^{k} \zeta_i \tag{3.5}$$

and

$$\Pi_{\delta}\left(\delta | \gamma, \mathbf{y}\right) \propto \delta^{a_2 - 1} \exp\left(-\left[b_2 \delta + \sum_{i=1}^{k} \left(\xi_i - \log\left(\xi_i\right)\right) + \sum_{i=1}^{d} S_i \xi_i + S^* \xi_k\right]\right) \prod_{i=1}^{k} \zeta_i, \tag{3.6}$$

respectively.

As expected, the conditional distributions $\Pi_{\gamma}(\cdot)$ and Π_{δ} of δ and γ given in (3.5) and (3.6), respectively, cannot be expressed in closed analytical forms corresponding to any well-known standard distributions. However, visual inspection in Figure 2 suggests that these conditional densities exhibit approximately normal behavior. Posterior inference for the model parameters is conducted using an iterative Metropolis–Hastings MCMC sampler (Algorithm 1), which facilitates the estimation of Bayesian point estimators as well as the construction of credible intervals.

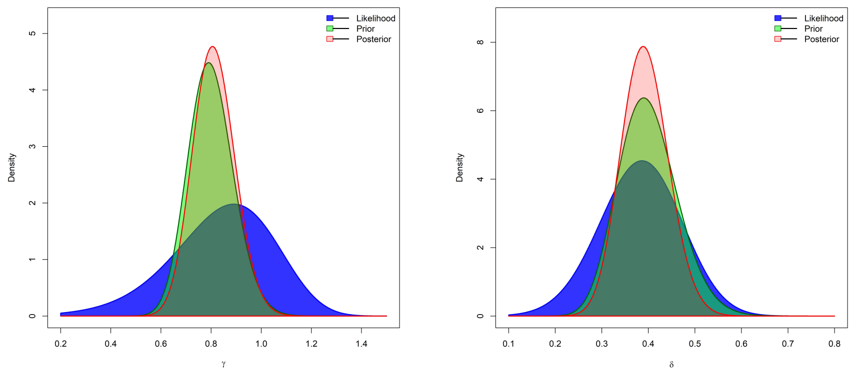

(a) At VFW$(0.8, 0.4)$

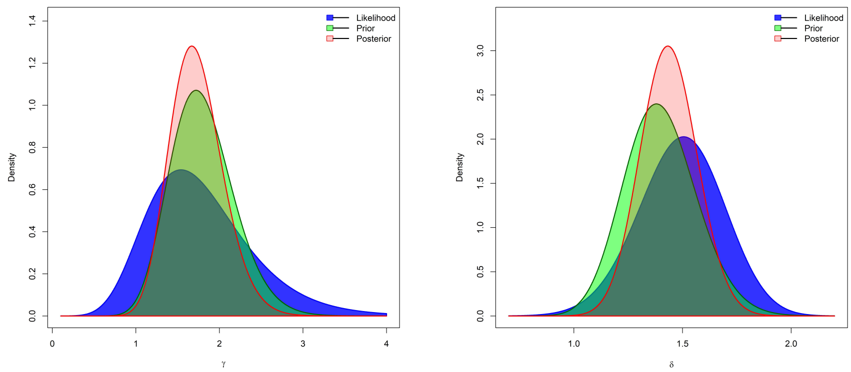

(b) At VFW$(1.8, 1.4)$

Figure 2. The posterior, prior, and likelihood density shapes of the VFW parameters γ (left) and δ (right).

Algorithm 1 The MCMC sampling for γ, δ, $R(t)$, and $h(t)$

Input: Initial estimates $\hat{\gamma}$, $\hat{\delta}$, number of iterations $\wp$, and burn-in $\wp^\star$.
Initialize:
$\gamma^{(0)} \leftarrow \hat{\gamma}, \quad \delta^{(0)} \leftarrow \hat{\delta}$
$j \leftarrow 1$
for $j = 1$ to $\wp$ **do**
    Generate proposal values:
    $\gamma^* \sim N(\hat{\gamma}, \hat{\varepsilon}_{11})$
    $\delta^* \sim N(\hat{\delta}, \hat{\varepsilon}_{22})$
    Compute acceptance ratios:
    $\kappa_\gamma \leftarrow \dfrac{\Pi_\gamma(\gamma^* \mid \delta^{(j-1)}, \mathbf{y})}{\Pi_\gamma(\gamma^{(j-1)} \mid \delta^{(j-1)}, \mathbf{y})}$
    $\kappa_\delta \leftarrow \dfrac{\Pi_\delta(\delta^* \mid \gamma^{(j)}, \mathbf{y})}{\Pi_\delta(\delta^{(j-1)} \mid \gamma^{(j)}, \mathbf{y})}$
    Generate $u_i \sim U(0, 1)$ (for $i = 1, 2$)
    if $u_1 \le \min(1, \kappa_\gamma)$ **then**
        $\gamma^{(j)} \leftarrow \gamma^*$
    else
        $\gamma^{(j)} \leftarrow \gamma^{(j-1)}$
    end if
    if $u_2 \le \min(1, \kappa_\delta)$ **then**
        $\delta^{(j)} \leftarrow \delta^*$
    else
        $\delta^{(j)} \leftarrow \delta^{(j-1)}$
    end if
    Compute $R^{(j)}(t)$ and $h^{(j)}(t)$ for $t > 0$ by replacing γ and δ with $\gamma^{(j)}$ and $\delta^{(j)}$, respectively.
end for
Compute Bayes estimates of γ, δ, $R(t)$, or $h(t)$ (say, ω):

$$\tilde{\omega}_{MH} = \frac{1}{\wp - \wp^\star} \sum_{j=\wp^\star+1}^{\wp} \omega^{(j)}.$$

Compute the $100(1-\varphi)\%$ BCI for ω:
Order $\omega^{(j)}$ for $j = \wp^\star + 1, \ldots, \wp$ as $\omega_{(\wp^\star+1)}, \omega_{(\wp^\star+2)}, \ldots, \omega_{(\wp)}$.

$$\text{BCI} = \left\{\omega_{((\wp-\wp^\star)\frac{\varphi}{2})},\ \omega_{((\wp-\wp^\star)(1-\frac{\varphi}{2}))}\right\}.$$

Compute the $100(1-\varphi)\%$ HPD interval of ω:

$$\text{HPD} = \left\{\omega_{(j^*)},\ \omega_{(j^*+(\wp-\wp_0)(1-\varphi))}\right\},$$

where j^* minimizes

$$\omega_{(j+[(\wp-\wp_0)(1-\varphi)])} - \omega_{(j)}.$$

4. Monte Carlo comparisons

This part provides the complete Monte Carlo simulations to analyze the performance and efficiency of the obtained point and interval estimators for γ, δ, $R(t)$, and $h(t)$ established in the prior sections.

4.1. Simulation designs

The performance of the proposed point and interval estimators for γ, δ, $R(t)$, and $h(t)$ is analyzed across a series of controlled experimental scenarios defined by the threshold level T, the total number of test items n, the effective sample size k, and the progressive censoring scheme $\mathbf{S}$. These factors are systematically varied to assess the robustness and sensitivity of the estimators under different testing conditions. To achieve this objective, a total of 1000 simulated datasets are generated from two distinct populations governed by the VFW lifetime distribution; namely, Set A: VFW$(0.8, 0.4)$ and Set B: VFW$(1.8, 1.4)$. At $t = 0.25$, the value of $(R(t),\ h(t))$ is $(0.9793,\ 0.3432)$ for Set A and $(0.9796,\ 0.3460)$ for Set B, respectively, serving as benchmarks for performance comparison.

Table 1. Different removals in Monte Carlo simulations.

Design	(n, k)	Design	(n, k)
	(30,10)		(30,20)
[1]	$(5^{[4]},0^{[6]})$	[1]	$(5^{[2]},0^{[18]})$
[2]	$(0^{[3]},5^{[4]},0^{[3]})$	[2]	$(0^{[9]},5^{[2]},0^{[9]})$
[3]	$(0^{[6]},5^{[4]})$	[3]	$(0^{[18]},5^{[2]})$
	(50,20)		(50,40)
[1]	$(5^{[6]},0^{[14]})$	[1]	$(5^{[2]},0^{[38]})$
[2]	$(0^{[7]},5^{[6]},0^{[7]})$	[2]	$(0^{[19]},5^{[2]},0^{[19]})$
[3]	$(0^{[14]},5^{[6]})$	[3]	$(0^{[38]},5^{[2]})$
	(80,30)		(80,60)
[1]	$(5^{[10]},0^{[20]})$	[1]	$(5^{[4]},0^{[56]})$
[2]	$(0^{[10]},5^{[10]},0^{[10]})$	[2]	$(0^{[28]},5^{[4]},0^{[28]})$
[3]	$(0^{[20]},5^{[10]})$	[3]	$(0^{[56]},5^{[4]})$

To ensure a comprehensive performance assessment, we set $n \in \{30,\ 50,\ 80\}$, while the threshold level T is examined at $T \in \{0.5,\ 1.5\}$. In addition, several effective sample sizes k and alternative progressive censoring schemes $\mathbf{S}$ are investigated, where the censoring pattern $\mathcal{S} : (0, 0, 0, 1, 1, 1)$ as an example is denoted as $(0^{[3]}, 1^{[3]})$ for brevity, as detailed in Table 1. The values selected for T, n, k, and $\mathbf{S}$ are intended to represent practical reliability-testing scenarios encountered in engineering and life-testing experiments. In practice, the sample size of n is moderate due to cost and time constraints associated with reliability experiments. The item k represents the number of observed failures required to terminate the experiment, while T and $\mathbf{S}$ correspond to termination threshold and removal design, respectively. By considering different combinations of these quantities, the simulation study reflects a range of practical experimental conditions under which progressive censoring schemes are typically implemented in reliability analysis. Every one of these combinations is carefully designed to account for the effects of censoring severity and sample strategy on estimator validity and precision. The complete algorithmic steps for generating and analyzing the simulated datasets under these configurations are provided in Algorithm 2. This systematic setup ensures the reproducibility and comparability of results across all simulated conditions, thereby providing a rigorous validation of the proposed inferential procedures.

Algorithm 2 Simulate the T2A-PC dataset from VFW(γ, δ)

1: Initialize parameters γ and δ.
2: Generate an ordinary T2-PC sample:

   1. Draw k uniform random numbers $v_1, v_2, \ldots, v_k$.
   2. For $i = 1$ to k: $a_i \leftarrow v_i^{(i+\sum_{j=k-i+1}^{k} S_j)^{-1}}$
   3. Find: $U_i \leftarrow 1 - (a_k a_{k-1} \cdots a_{k-i+1})$
   4. Get: $Y_i \leftarrow G^{-1}(u_i; \gamma, \delta)$

3: Determine d at T and discard Y_i for $i = d+2, \ldots, k$.
4: Generate $(k-d-1)$ order statistics $\{Y_{d+2}, \ldots, Y_k\}$ from truncated distribution $f(y)/R(Y_{d+1})$ with sample size $n - d - 1 - \sum_{i=1}^{d} S_i$.
5: Determine T2A-PC sample type:

   1. If $Y_k < T$, set $\mathbf{S} = (S_1, S_2, \ldots, S_k)$, stop at Y_k (Case 1)
   2. If $T < Y_k$, set $\mathbf{S} = (S_1, S_2, \ldots, S_d, 0, \ldots, 0, S_k)$, stop at Y_k (Case 2)

We disregard the Bayes estimate in addition to the associated BCI/HPD estimates for each parameter, and we generate $\wp = 12000$ MCMC iterations (by $\wp^\star = 2000$). Accordingly, the remaining 10000 iterations are used to obtain the Bayesian evaluations for γ, δ, $R(t)$, and $h(t)$. Two packages are utilized: (i) The maxLik package (Henningsen and Toomet [18]) for likelihood estimates through NA-based and NL-based methods, and (ii) the coda package (Plummer et al. [22]) for obtaining Bayesian estimates and the associated BCI/HPD results.

To explore the influence of prior specification on the Bayesian results, two informative gamma prior sets for α, defined by the hyperparameters (a_i, b_i) for $i = 1, 2$, are assigned based on the mean/variance approach presented by Kundu [21]. Subsequently, the hyperparameter values of $(a_1,\ b_1,\ a_2,\ b_2)$ are specified as follows:

(a) Set 1: Prior A: (4, 5, 2, 5); Prior B: (8, 10, 4, 10);
(b) Set 2: Prior A: (9, 5, 7, 5); Prior B: (18, 10, 14, 10).

To examine how prior choices affect Bayesian estimation, we conduct a sensitivity analysis of the posterior distributions of γ and δ under different prior specifications. The goal is to determine the extent to which posterior summaries, such as means, standard deviations, and credible intervals, are influenced by the selected prior, especially in challenging scenarios such as censored data. Based on the T2A-PC datasets generated from Sets A and B, we evaluate the robustness of the posterior densities in (3.5) and (3.6) across four types of priors: Informative, improper, overdispersed, and weak (see Figure 3). The results show that the informative gamma prior with parameters (a_i, b_i) for $i = 1, 2$

yields more concentrated and stable posterior distributions, typically centered near the prior mean. By comparison, the remaining priors allow the data to exert a stronger influence, leading to broader credible intervals and higher posterior variability, with the overdispersed prior generating the largest dispersion and noticeable bias. Overall, the analysis demonstrates that posterior conclusions can be substantially affected by prior selection, particularly when the effective sample size is small.

On the other hand, for interval estimation results, two different accuracy metrics are employed:

i) Average Interval Length (AIL):

$$\text{AIL}_{95\%}(\chi) = \frac{1}{1000}\sum_{i=1}^{1000}\left(\mathcal{U}_{\ddot{\chi}_j^{(i)}} - \mathcal{L}_{\ddot{\chi}_j^{(i)}}\right), \quad j = 1, 2, 3, 4;$$

ii) Coverage Probability (CP):

$$\text{CP}_{95\%}(\chi) = \frac{1}{1000}\sum_{i=1}^{1000}\aleph_{\left(\mathcal{L}_{\ddot{\chi}_j^{(i)}};\mathcal{U}_{\ddot{\chi}_j^{(i)}}\right)}(\chi_j), \quad j = 1, 2, 3, 4,$$

where $\aleph(\cdot)$ is the indicator function.

For practical calculations, the accuracy of the point estimators is examined using the following criteria:

i) Root Mean Squared Error (RMSE):

$$\text{RMSE}(\ddot{\chi}_j) = \sqrt{\frac{1}{1000}\sum_{i=1}^{1000}\left(\ddot{\chi}^{(i)} - \chi_j\right)^2}, \quad j = 1, 2, 3, 4;$$

ii) Average Relative Absolute Bias (ARAB):

$$\text{ARAB}(\ddot{\chi}_j) = \frac{1}{1000}\sum_{i=1}^{1000}\chi_j^{-1}|\ddot{\chi}_j^{(i)} - \chi_j|, \quad j = 1, 2, 3, 4,$$

where $\ddot{\chi}^{(i)}$ represents the ith replication, with $\chi_1 = \gamma, \chi_2 = \delta, \chi_3 = R(t)$, and $\chi_4 = h(t)$.

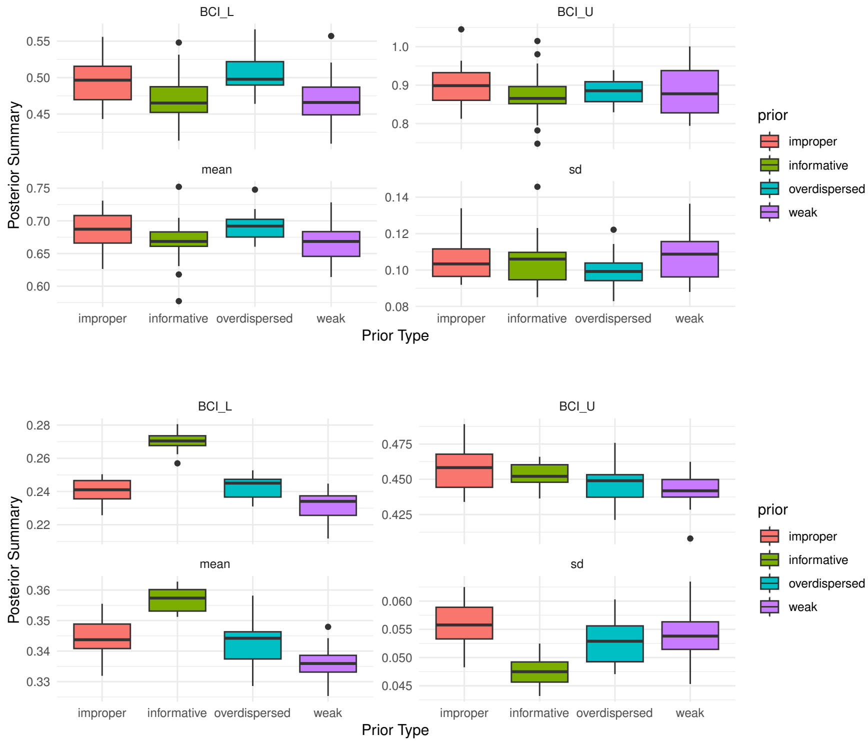

(a) Set A

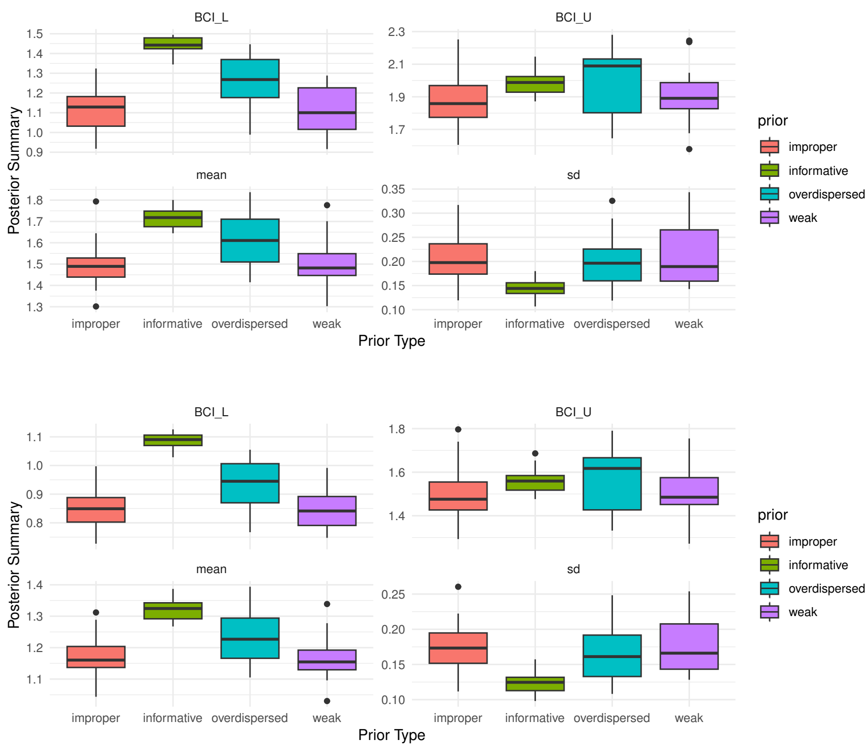

(b) Set B

Figure 3. Sensitivity of four prior choices on the posterior results of γ (top) and δ (bottom).

4.2. Simulation outputs and discussions

From Tables S1–S8, several important observations can be drawn regarding the estimators' performance of γ, δ, $R(t)$, and $h(t)$. The conclusions are summarized as follows:

- The proposed estimators exhibit consistent and satisfactory performance across all simulation settings, as reflected by their relatively low RMSE, ARAB, and AIL values and high CP values.
- Increasing the total sample size n (or effective sample size k) enhances the estimation precision, while a reduction in the number of removals produces a similar improvement. Additionally, increasing the level of T generally improves the accuracy of the estimates for γ, δ, $R(t)$, and $h(t)$.
- Bayesian estimators based on Prior B consistently outperform those based on Prior A, while both Bayesian methods demonstrate superiority over the classical likelihood-based estimators in terms of bias reduction and precision.
- Across both informative prior specifications, the HPD provides more efficient estimates than the BCI.
- When comparing different interval estimation techniques:
  - For all parameters, the 95% HPD intervals exhibit the best overall performance and are nearly indistinguishable from the corresponding 95% BCI intervals, both of which outperform the proposed ACI methods;
  - for γ and $h(t)$, the ACI-NA method yields better results than the ACI-NL method;
  - for δ and $R(t)$, the ACI-NL method performs better than the ACI-NA method;
  - the CP values for all VFW parameters and reliability characteristics obtained from the BCI/HPD and ACI-NA/ACI-NL methods are close to (or exceed) the nominal 95% level in most settings.
- As the actual values of γ and δ increase:
  - For both maximum likelihood and Bayesian methods, the RMSEs and ARABs of γ increase, whereas those of δ, $R(t)$, and $h(t)$ tend to decrease;
  - regarding interval estimates (ACI-NA/ACI-NL and BCI/HPD), the AILs of γ, δ, $R(t)$, and $h(t)$ increase with corresponding decreases in CP.
- It can be better noticed here that all calculated MLEs exhibit stable convergence across all investigated censoring configurations, and their estimation accuracy improves as the sample size increases from smaller to larger values of n. Additionally, the Bayesian estimators obtained via the MCMC-based algorithm also show stable performance, and their associated BCI and HPD results often achieve CPs close to the nominal 95% level, typically fluctuating around 0.94–0.97 across most scenarios.
- Considering the proposed censoring schemes $[i]$, $i = 1, 2, 3$:
  - Scheme [3] (right censoring) yields more accurate estimates for γ.
  - Scheme [2] (middle censoring) provides more precise estimates for δ and $R(t)$.
  - Scheme [1] (left censoring) produces more accurate estimates for $h(t)$.
- We can clarify the practical significance of the simulation results from a reliability practice perspective. In engineering applications, life-testing experiments are often conducted under time and cost constraints, which lead to progressively or hybrid censored samples rather than complete data.

- All results demonstrate how the proposed estimation procedures perform under such realistic conditions, allowing practitioners to identify methods that provide stable parameter estimates and reliable confidence intervals even with limited or censored observations. Consequently, these findings can assist reliability engineers in selecting appropriate estimation techniques when analyzing lifetime data from laboratory life tests, maintenance studies, or accelerated reliability experiments conducted under the plan investigated.
- Overall, the Bayesian estimation approach implemented via the Metropolis–Hastings algorithm is recommended for analyzing the VFW model under progressive T2A-PC, as it consistently provides more efficient and reliable inference than its frequentist competitor.

5. Real-world data applications

This section illustrates the practical applicability of the proposed methods through two empirical case studies derived from engineering and physical datasets.

5.1. Carbon fibers data analysis

This study examines the tensile strength of carbon fibers, measured in gigapascals (GPa), when subjected to uniaxial tension at a gauge length of 20 mm (see Table 2). Tensile strength represents the maximum stress a fiber can withstand before failure, providing a key indicator of its mechanical performance; see Ahmed and Al-Essa [23].

Table 2. Tensile strength (in GPa) of 69 carbon fibers.

0.1312	0.1314	0.1479	0.1552	0.1700	0.1803	0.1861	0.1865	0.1944	0.1958
0.1966	0.1997	0.2006	0.2021	0.2027	0.2055	0.2063	0.2098	0.2140	0.2179
0.2224	0.2240	0.2253	0.2270	0.2272	0.2274	0.2301	0.2301	0.2359	0.2382
0.2382	0.2426	0.2434	0.2435	0.2478	0.2490	0.2511	0.2514	0.2535	0.2554
0.2566	0.2570	0.2586	0.2629	0.2633	0.2642	0.2648	0.2684	0.2697	0.2726
0.2770	0.2773	0.2800	0.2809	0.2818	0.2821	0.2848	0.2880	0.2954	0.3012
0.3067	0.3084	0.3090	0.3096	0.3128	0.3233	0.3433	0.3585	0.3585	

We begin by comparing the proposed VFW distribution, fitted to the complete carbon fiber dataset, against twelve competing lifetime models exhibiting diverse hazard rate behaviors (see Table 3). To identify the most suitable model, eight model selection criteria are employed: (1) Negative log-likelihood (NLL), (2) Akaike information (AI), (3) Bayesian information (BI), (4) consistent AI (CAI), (5) Hannan-Quinn information (HQI), and (6) the Kolmogorov-Smirnov (KS) statistic along with its associated P-value. The fitted metrics (1)–(6) were via the AdequacyModel package (by Marinho et al. [24]); the corresponding results are summarized in Table 4.

In addition, the MLEs of each model parameter, along with their associated standard errors (Std.Ers), are also presented in Table 4. Since the most appropriate distribution is expected to exhibit the smallest values of all model selection criteria, with the exception of the largest P-value for the KS statistic, the results in Table 4 indicate that the VFW model outperforms the alternative candidates.

Table 3. Competitive models of the VFW distribution.

Model	Symbol	Author(s)
New Extended Weibull	NEW(α, γ, δ)	Peng and Yan [25]
Power Generalized Weibull	PGW(α, γ, δ)	Bagdonavicius and Nikulin [26]
Harris-Extended-Exponential	HEE(α, γ, δ)	Pinho et al. [27]
Exponentiated-Pham	EP(α, γ, δ)	Alotaibi et al. [28]
Exponentiated-Weibull	EW(α, γ, δ)	Mudholkar and Srivastava [4]
Weibull-Exponential	WE(α, γ, δ)	Oguntunde et al. [29]
Gompertz-Makeham	GM(α, γ, δ)	Marshall and Olkin [30]
Alpha-Power-Exponential	APE(γ, δ)	Mahdavi and Kundu [31]
Generalized-Exponential	GE(γ, δ)	Gupta and Kundu [32]
Birnbaum-Saunders	BS(γ, δ)	Birnbaum and Saunders [33]
Weibull	W(γ, δ)	Weibull [34]
Gamma	G(γ, δ)	Johnson et al. [35]

Table 4. Fitting summary of the VFW model and its competitors from carbon fiber data.

Model	α		γ		δ		NLL	AI	CAI	BI	HQI	KS	*P*-value
	Est.	Std.Er	Est.	Std.Er	Est.	Std.Er							
VFW	-	-	0.4122	0.1383	6.6196	1.1359	-110.006	-216.011	-215.830	-211.543	-214.239	0.0420	0.9997
PGW	34.419	19.613	3.9535	0.3089	3.9783	1.5608	-106.570	-207.139	-206.770	-200.437	-204.480	0.0882	0.6568
NEW	1.4512	0.5953	0.4360	2.1452	147.35	110.53	-109.479	-212.958	-212.589	-206.256	-210.299	0.0505	0.9946
APE	-	-	122.95	47.819	8.9962	0.6308	-68.018	-132.036	-131.855	-127.568	-130.264	0.3139	0.0002
HEE	0.6507	0.2417	32.212	9.4476	243.06	84.125	-102.164	-198.328	-197.959	-191.625	-195.669	0.1637	0.0495
WE	23.724	49.493	4.5287	0.4714	1.5165	0.5224	-108.810	-211.619	-211.250	-204.917	-208.960	0.0624	0.9509
EW	4.3068	0.6066	2.0269	1.2974	3.8633	1.2278	-110.002	-214.037	-213.668	-207.335	-211.378	0.0424	0.9992
EP	0.7831	0.1843	96.263	73.899	22.342	15.098	-108.574	-211.148	-210.779	-204.446	-208.489	0.0616	0.9562
GE	-	-	78.857	28.722	19.847	1.7344	-104.213	-204.427	-204.245	-199.959	-202.654	0.0928	0.5923
BS	-	-	0.2153	0.0185	0.2400	0.0062	-107.411	-210.822	-210.640	-206.354	-209.049	0.0717	0.8697
W	-	-	3.8030	0.2320	152.04	44.109	-101.954	-199.909	-199.727	-195.440	-198.136	0.1431	0.1184
G	-	-	23.204	3.9225	94.622	16.169	-108.840	-213.680	-213.498	-209.212	-211.907	0.0577	0.9757

Figure 4 presents several graphical diagnostics used to evaluate the fit of the VFW model relative to its competing distributions for the carbon fiber dataset. The graphical analyses include (i) plots of empirical and fitted RF/PDF lines together with probability–probability (P–P) and quantile–quantile (Q–Q) plots, (ii) the scaled total time on test (TTT) transformation, and (iii) the log-likelihood contour plot. Overall, the graphical results displayed in Figures 4(a)–(d) provide consistent visual confirmation of the VFW model's adequacy.

In addition, Figure 4(e) illustrates a clear increasing failure rate (IFR) pattern, aligning closely with the theoretical hazard rate behavior expected from the VFW distribution. Figure 4(f) indicates that the ML estimates, $\hat{\gamma} \approx 0.4122$ and $\hat{\delta} \approx 6.6196$, exist and are unique. Accordingly, the estimated values of $\hat{\gamma}$ and $\hat{\delta}$ are adopted as suitable initial values for all subsequent computations of γ, δ, $R(t)$, and $h(t)$ involving the carbon fiber data.

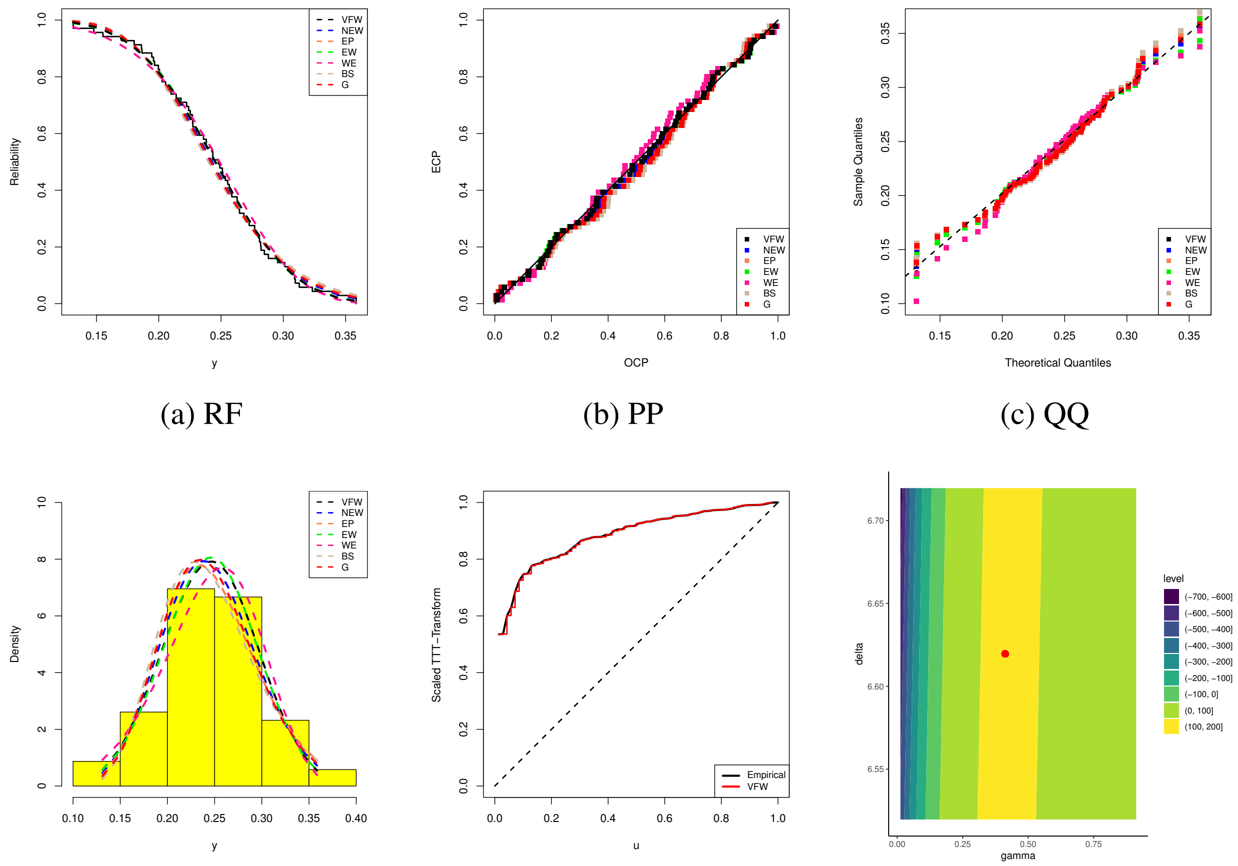

(a) RF (b) PP (c) QQ

(d) PDF (e) TTT (f) Contour

Figure 4. Fitting diagrams for the VFW model from carbon fiber data.

Now, various T2A-PC samples are generated from the carbon fiber dataset summarized in Table 2, using a fixed sample size of $k = 29$ and various combinations of censoring schemes $\mathbf{S}$ and threshold values T (see Table 5). For each sample $\mathcal{S}[i]$ $(i = 1, 2, 3)$, the frequentist and Bayesian MCMC estimates (along with their corresponding Std.Ers), as well as the 95% ACI-NA/ACI-NL and BCI/HPD interval estimates (with their respective Int.Ls), of γ, δ, $R(t)$, and $h(t)$ at $t = 0.01$ are reported in Table 6. Since no prior information is available on the parameters of the VFW(γ, δ) distribution from the carbon fiber dataset, the Bayesian estimates and their credible intervals are obtained via an MCMC sampler with 40,000 iterations, discarding the initial 10,000 as burn-in, under improper gamma priors. When compared to the classical likelihood-based estimates, the Bayesian approach using an improper gamma prior demonstrates superior performance, as evidenced by smaller standard errors and narrower interval lengths.

Table 5. Different T2A-PC samples from carbon fiber data.

Sample	**S**	$T(d)$	S^*	Censored Data
$\mathcal{S}[1]$	$(5^{[8]}, 0^{[21]})$	0.35(29)	0	0.1312, 0.1479, 0.1700, 0.1861, 0.1944, 0.1997, 0.2006, 0.2098, 0.2140, 0.2224, 0.2240, 0.2272, 0.2301, 0.2382, 0.2426, 0.2435, 0.2478, 0.2490, 0.2511, 0.2554, 0.2570, 0.2586, 0.2629, 0.2642, 0.2770, 0.2821, 0.2848, 0.3090, 0.3433
$\mathcal{S}[2]$	$(0^{[10]}, 5^{[8]}, 0^{[11]})$	0.25(16)	10	0.1314, 0.1479, 0.1552, 0.1700, 0.1803, 0.1861, 0.1865, 0.1944, 0.1958, 0.1966, 0.1997, 0.2006, 0.2021, 0.2098, 0.2140, 0.2274, 0.2382, 0.2514, 0.2566, 0.2629, 0.2697, 0.2773, 0.2800, 0.2809, 0.2848, 0.2880, 0.3084, 0.3090, 0.3128
$\mathcal{S}[3]$	$(0^{[21]}, 5^{[8]})$	0.26(27)	20	0.1314, 0.1479, 0.1552, 0.1700, 0.1803, 0.1861, 0.1865, 0.1944, 0.1958, 0.1966, 0.1997, 0.2006, 0.2021, 0.2027, 0.2055, 0.2063, 0.2098, 0.2140, 0.2179, 0.2224, 0.2240, 0.2253, 0.2274, 0.2382, 0.2426, 0.2478, 0.2535, 0.2633, 0.2726

Table 6. Estimates of γ, δ, $R(t)$, and $h(t)$ from carbon fiber data.

Sample	Par.	MLE		MCMC		ACI-NA ACI-NL			BCI HPD		
		Est.	Std.Er	Est.	Std.Er	Low.	Upp.	Int.L	Low.	Upp.	Int.L
$\mathcal{S}[1]$	γ	0.70180	0.21523	0.70378	0.02975	0.27996	1.12364	0.84368	0.64811	0.76483	0.11672
						0.38474	1.28015	0.89541	0.64699	0.76351	0.11653
	δ	9.82421	2.72723	9.82328	0.05023	4.47893	15.1695	10.6905	9.72423	9.92161	0.19737
						5.70166	16.9275	11.2259	9.72164	9.91806	0.19642
	$R(t)$	0.85109	0.03775	0.85073	0.02069	0.77711	0.92507	0.14796	0.80668	0.88792	0.08124
						0.78023	0.92838	0.14815	0.80990	0.89013	0.08023
	$h(t)$	5.82727	1.32959	5.85238	0.89304	3.22133	8.43321	5.21188	4.27530	7.78056	3.50527
						3.72606	9.11340	5.38734	4.18473	7.63602	3.45129
$\mathcal{S}[2]$	γ	0.17213	0.21929	0.16533	0.01079	0.00577	0.60193	0.59616	0.14891	0.18184	0.03294
						0.01417	2.09047	2.07630	0.14869	0.18130	0.03261
	δ	4.08019	1.17261	4.07997	0.00796	1.78193	6.37846	4.59654	4.06448	4.09576	0.03128
						2.32302	7.16651	4.84348	4.06399	4.09521	0.03122
	$R(t)$	0.86199	0.03608	0.85746	0.00722	0.79127	0.93271	0.14144	0.84588	0.86812	0.02224
						0.79409	0.93569	0.14160	0.84606	0.86818	0.02211
	$h(t)$	4.10808	0.85982	4.24190	0.21351	2.42287	5.79330	3.37042	3.92689	4.58435	0.65745
						2.72574	6.19149	3.46575	3.92143	4.57477	0.65334
$\mathcal{S}[3]$	γ	0.05220	0.25432	0.05203	0.00026	0.00250	0.55065	0.54815	0.05164	0.05242	0.00078
						0.00107	1.17690	1.17583	0.05165	0.05243	0.00078
	δ	3.38520	1.20640	3.38520	0.00020	1.02069	5.74970	4.72902	3.38480	3.38558	0.00079
						1.68359	6.80663	5.12304	3.38480	3.38559	0.00078
	$R(t)$	0.85947	0.03346	0.85936	0.00017	0.79389	0.92505	0.13116	0.85910	0.85962	0.00052
						0.79633	0.92762	0.13129	0.85909	0.85961	0.00052
	$h(t)$	3.90895	0.73314	3.91188	0.00461	2.47202	5.34587	2.87385	3.90494	3.91889	0.01395
						2.70653	5.64555	2.93901	3.90524	3.91910	0.01386

To further investigate the behavior of the LF surface and the dependence structure between the VFW model parameters, contour plots of the objective function over the parameter space are presented. These plots provide a visual assessment of the optimization landscape associated with the estimation procedure. The contours exhibit an existing minimum region, indicating the presence of a unique and stable solution for the MLEs of γ and δ. To verify the existence and uniqueness of the proposed MLEs of γ and δ, Figure 5 displays the log-likelihood contours for both parameters across all samples $\mathcal{S}[i]$ $(i = 1, 2, 3)$ summarized in Table 5. The profiles clearly indicate that, for each carbon fiber dataset, the MLEs of γ and δ exist and are unique. To further assess the convergence behavior of the Bayesian MCMC algorithm, Figure 6 presents the corresponding density and trace plots of γ, δ, $R(t)$, and $h(t)$ for the representative sample $\mathcal{S}[1]$. In these plots, the solid line represents the posterior mean (Bayes point estimate), whereas the dashed lines denote the 95% BCI limits.

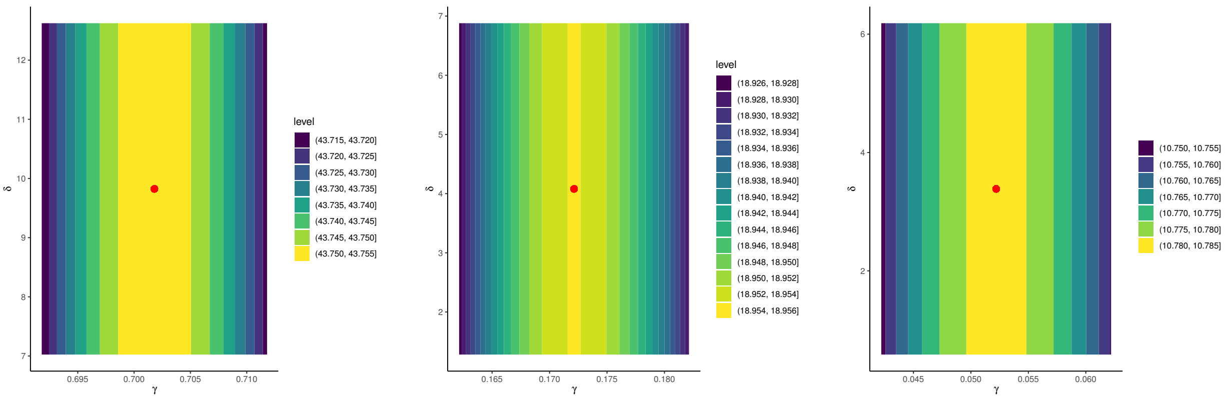

(a) $\mathcal{S}[1]$ (b) $\mathcal{S}[2]$ (c) $\mathcal{S}[3]$

Figure 5. Contours of γ (left) and δ (right) from carbon fiber data.

The results demonstrate satisfactory convergence of the MCMC chains, confirming that the selected burn-in length is sufficient to remove the influence of initial values. Additionally, the posterior distributions of γ and δ appear approximately symmetric from $\mathcal{S}[i]$, $i = 1, 2, 3$, while those of $R(t)$ and $h(t)$ exhibit negative and positive skewness, respectively, based on $\mathcal{S}[1]$ as well as both being symmetrical based on $\mathcal{S}[i]$, $i = 2, 3$. Descriptive summaries—including the mean, mode, median, quartiles (Q_i, $i = 1, 2, 3$), standard deviation (Std.D), and skewness (Skew.)—based on 30,000 MCMC samples of γ, δ, $R(t)$, and $h(t)$ are reported in Table 7. These summaries further validate the results in Table 6 and align with the convergence patterns observed in Figure 6.

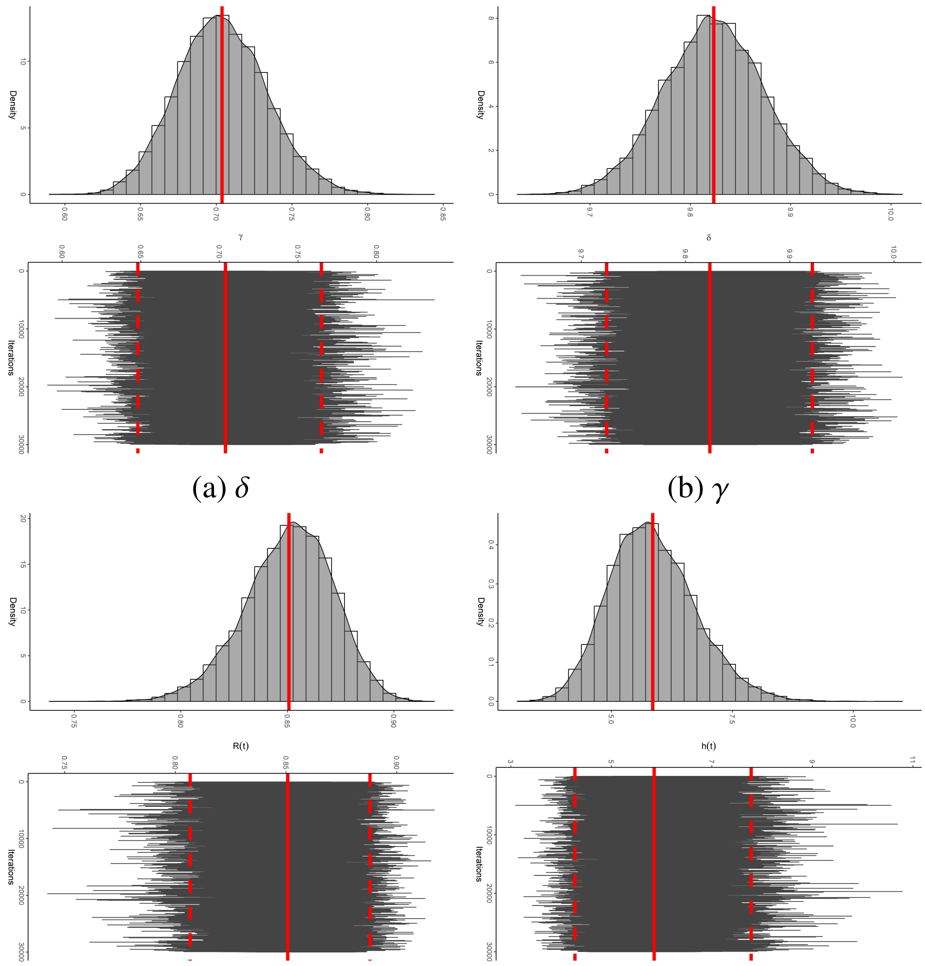

(a) δ (b) γ (c) $R(t)$ (d) $h(t)$

Figure 6. MCMC plots of γ, δ, $R(t)$, and $h(t)$ from carbon fiber data.

Table 7. Summary for 30,000 MCMC iterations of γ, δ, $R(t)$, and $h(t)$ from carbon fiber data.

Sample	Par.	Mean	Mode	Q_1	Q_2	Q_3	Std.D	Skew.
$\mathcal{S}[1]$	γ	0.70378	0.70252	0.68336	0.70285	0.72351	0.02968	0.16923
	δ	9.82328	9.82131	9.78937	9.82310	9.85733	0.05022	0.00353
	$R(t)$	0.85073	0.85172	0.83735	0.85189	0.86531	0.02069	-0.34655
	$h(t)$	5.85238	5.79971	5.22217	5.79170	6.42133	0.89271	0.41589
$\mathcal{S}[2]$	γ	0.16533	0.14589	0.15954	0.16531	0.17103	0.00838	0.03298
	δ	4.07997	4.07718	4.07456	4.07995	4.08530	0.00796	0.02470
	$R(t)$	0.85746	0.84425	0.85362	0.85760	0.86140	0.00562	-0.09934
	$h(t)$	4.24190	4.63073	4.12551	4.23789	4.35524	0.16637	0.10254
$\mathcal{S}[3]$	γ	0.05203	0.05137	0.05190	0.05203	0.05216	0.00020	-0.00317
	δ	3.38520	3.38521	3.38506	3.38520	3.38533	0.00020	0.00489
	$R(t)$	0.85936	0.85893	0.85927	0.85936	0.85945	0.00013	0.00852
	$h(t)$	3.91188	3.92345	3.90952	3.91191	3.91425	0.00355	-0.01024

5.2. *Flood data analysis*

The Susquehanna River in Harrisburg, PA, plays a vital role in the environmental, economic, and social landscape of the mid-Atlantic region of the United States. Flowing through Pennsylvania's capital, the river provides essential resources for water supply, transportation, and recreation, while sustaining diverse and dynamic aquatic ecosystems. The maximum flood level at this location serves as a critical hydrological indicator for assessing flood potential and informing water resource management strategies. It represents the peak stage attainable under extreme hydrometeorological conditions and forms the basis for evaluating floodplain vulnerability and enhancing regional resilience planning. This application focuses on analyzing a real-world dataset that represents the twenty flood (high) levels for the Susquehanna River in Harrisburg, Pennsylvania; see Khalifa et al. [36].

Using the complete flood dataset listed in Table 8, we further assess the superiority of the VFW distribution by comparing its fit against the same twelve competing lifetime models listed in Table 3. Under the fitting configurations described in Table 4, the results summarized in Table 9 reveal that the VFW model provides the best overall performance, yielding the lowest values for all model selection criteria and the highest associated P-value among all others. Furthermore, the graphical analyses presented in Figures 7(a)–(d) support the goodness-of-fit results discussed earlier. In particular, Figure 7(e) illustrates an increasing failure rate (IFR) pattern for the flood dataset, consistent with the theoretical hazard rate behavior of the VFW distribution. Finally, Figure 7(f) confirms the existence and uniqueness of the MLEs for γ and δ. Consequently, the estimates $\hat{\gamma} \approx 0.8267$ and $\hat{\delta} \approx 1.7199$ are adopted as initial values for all subsequent analyses of the proposed estimators.

Table 8. Maximum flood level for the Susquehanna River.

0.265	0.269	0.297	0.315	0.324	0.338	0.379	0.379	0.392	0.402
0.412	0.416	0.418	0.423	0.449	0.484	0.494	0.613	0.654	0.740

Table 9. Fitting summary of the VFW model and its competitors from flood data.

Model	α		γ		δ		NLL	AI	CAI	BI	HQI	KS	P-value
	Est.	Std.Er	Est.	Std.Er	Est.	Std.Er							
VFW	-	-	0.3882	0.0284	3.4278	0.1534	-61.9573	-119.915	-119.209	-117.923	-119.526	0.1174	0.9456
PGW	51.401	821.51	2.3317	0.4183	15.993	236.95	-57.3740	-108.748	-107.248	-105.761	-108.165	0.2167	0.3046
NEW	0.2656	0.1165	2.1189	2.3371	0.5539	2.6022	-61.8630	-117.726	-116.226	-114.739	-117.143	0.1292	0.8922
APE	-	-	368.08	320.57	55.876	6.9283	-55.4035	-106.807	-106.101	-104.815	-106.418	0.2588	0.1372
HEE	0.9512	0.9783	133.15	92.236	165.64	127.71	-59.7639	-113.528	-112.028	-110.541	-112.945	0.1500	0.7593
WE	28.847	100.64	3.0264	0.5768	6.0333	5.3428	-58.9350	-111.870	-110.370	-108.883	-111.287	0.2035	0.3789
EW	49.764	28.591	11.417	14.366	1.4718	0.5760	-61.8286	-117.657	-116.157	-114.670	-117.074	0.1449	0.7950
EP	0.3222	0.0601	190.82	124.00	173.13	201.88	-61.9427	-117.989	-116.489	-115.001	-117.405	0.1556	0.7180
GE	-	-	52.323	38.561	107.23	20.577	-61.8635	-119.413	-118.707	-117.421	-119.024	0.1310	0.8827
BS	-	-	0.2739	0.0439	0.0403	0.0024	-61.8648	-119.730	-119.024	-117.738	-119.341	0.1306	0.8849
W	-	-	1.5358	0.1582	99.880	44.979	-50.3265	-96.6530	-95.9471	-94.6615	-96.2642	0.3150	0.0377
G	-	-	6.9693	2.1532	160.45	51.401	-59.5070	-115.014	-114.308	-113.023	-114.625	0.1772	0.5568

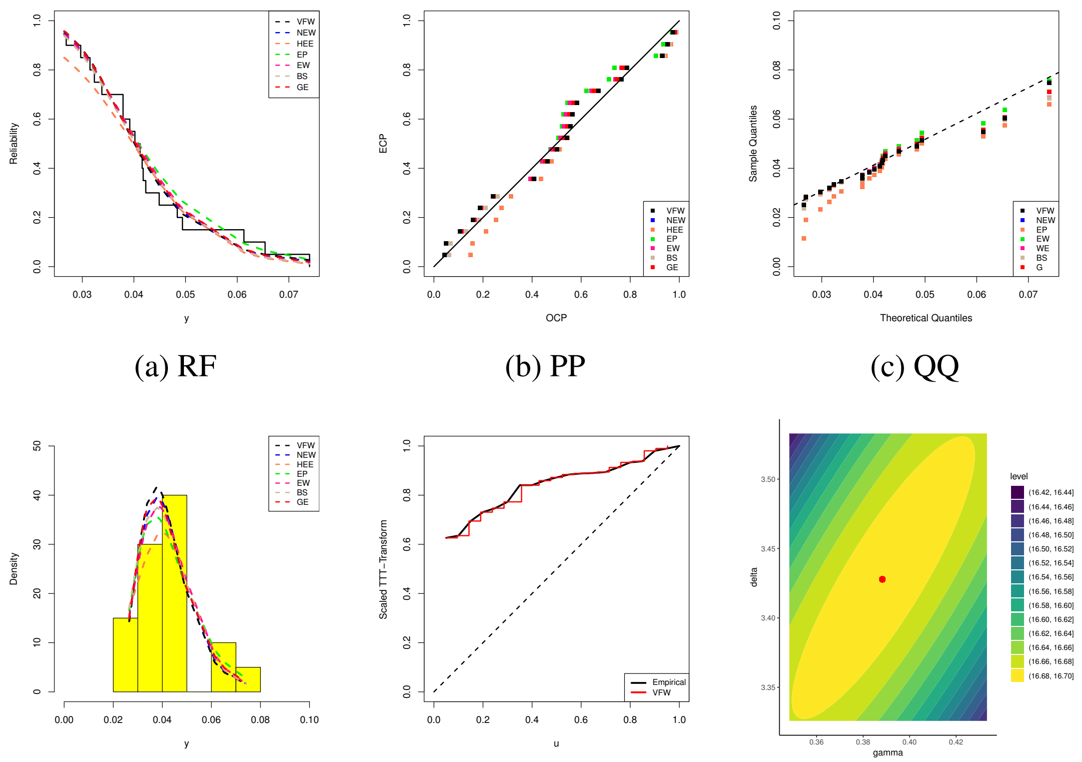

(a) RF (b) PP (c) QQ

(d) PDF (e) TTT (f) Contour

Figure 7. Fitting diagrams for the VFW model from flood data.

To investigate the practical performance of the proposed estimation procedures, a set of T2A-PC samples was generated from the flood dataset summarized in Table 8. The analysis was conducted using a fixed effective sample size of $k = 15$ and several combinations of censoring schemes $\mathbf{S}$ and threshold levels T (see Table 10). For each generated sample $\mathcal{S}[i]$ ($i = 1, 2, 3$), both frequentist and Bayesian MCMC estimates were obtained for γ, δ, $R(t)$, and $h(t)$ at $t = 0.01$, together with their corresponding standard errors. The associated 95% ACI-NA/ACI-NL and BCI/HPD interval estimates, along with their interval lengths, are reported in Table 11.

As no prior information on the VFW(γ, δ) parameters is available for this dataset, the Bayesian estimation was implemented under improper gamma priors using an MCMC sampler with 40,000 iterations, discarding the first 10,000 as burn-in. The results clearly demonstrate that the Bayesian procedure yields more precise inference compared to the classical likelihood-based approach, as evidenced by smaller standard errors and narrower interval estimates. This improvement reflects the robustness and efficiency of the Bayesian framework, even under noninformative prior assumptions.

Table 10. Different T2A-PC samples from flood data.

Sample	**S**	$T(d)$	S^*	Censored Data
$\mathcal{S}[1]$	$(1^{[5]}, 0^{[10]})$	0.065(15)	0	0.0265, 0.0269, 0.0297, 0.0324, 0.0338, 0.0379, 0.0379, 0.0392, 0.0402, 0.0412, 0.0416, 0.0418, 0.0449, 0.0494, 0.0613
$\mathcal{S}[2]$	$(0^{[5]}, 1^{[5]}, 0^{[5]})$	0.041(8)	2	0.0265, 0.0269, 0.0297, 0.0315, 0.0324, 0.0338, 0.0392, 0.0402, 0.0412, 0.0416, 0.0418, 0.0423, 0.0449, 0.0484, 0.0613
$\mathcal{S}[3]$	$(0^{[10]}, 1^{[5]})$	0.043(12)	3	0.0265, 0.0269, 0.0297, 0.0315, 0.0323, 0.0338, 0.0379, 0.0379, 0.0392, 0.0402, 0.0412, 0.0423, 0.0449, 0.0484, 0.0654

Table 11. Estimates of γ, δ, $R(t)$, and $h(t)$ from AML data.

Sample	Par.	MLE		MCMC		ACI-NA ACI-NL			BCI HPD		
		Est.	Std.Er	Est.	Std.Er	Low.	Upp.	Int.L	Low.	Upp.	Int.L
$\mathcal{S}[1]$	γ	0.85208	0.33337	0.85135	0.04714	0.19869	1.50547	1.30678	0.75953	0.94397	0.18444
						0.39578	1.83444	1.43866	0.75861	0.94274	0.18413
	δ	4.82936	1.17447	4.82899	0.04987	2.52744	7.13128	4.60384	4.73092	4.92709	0.19616
						2.99835	7.77851	4.78016	4.72793	4.92362	0.19568
	$R(t)$	0.97731	0.00904	0.97711	0.00216	0.95959	0.99503	0.03544	0.97243	0.98082	0.00839
						0.95975	0.99520	0.03545	0.97290	0.98120	0.00830
	$h(t)$	0.69353	0.27463	0.70011	0.06938	0.15527	1.23179	1.07652	0.58044	0.85022	0.26978
						0.31915	1.50705	1.18790	0.57054	0.83746	0.26692
$\mathcal{S}[2]$	γ	0.84676	0.35368	0.84571	0.04713	0.15355	1.53996	1.38642	0.75359	0.93954	0.18596
						0.37344	1.91999	1.54655	0.75273	0.93839	0.18566
	δ	4.72780	1.22375	4.72707	0.05007	2.32930	7.12631	4.79701	4.62871	4.82581	0.19710
						2.84665	7.85210	5.00545	4.62783	4.82447	0.19664
	$R(t)$	0.97766	0.00923	0.97745	0.00210	0.95956	0.99576	0.03620	0.97291	0.98110	0.00819
						0.95972	0.99592	0.03620	0.97320	0.98127	0.00807
	$h(t)$	0.68068	0.27858	0.68735	0.06708	0.13467	1.22669	1.09203	0.57032	0.83212	0.26181
						0.30519	1.51815	1.21296	0.56550	0.82403	0.25853
$\mathcal{S}[3]$	γ	0.60691	0.29815	0.60216	0.04775	0.02254	1.19127	1.16873	0.50980	0.69652	0.18672
						0.23172	1.58959	1.35787	0.50480	0.69138	0.18659
	δ	3.91184	0.86835	3.91055	0.04995	2.20989	5.61378	3.40389	3.81259	4.00890	0.19632
						2.53180	6.04410	3.51230	3.81248	4.00854	0.19607
	$R(t)$	0.97104	0.01260	0.97042	0.00344	0.94633	0.99574	0.04941	0.96295	0.97622	0.01327
						0.94665	0.99606	0.04941	0.96361	0.97662	0.01300
	$h(t)$	0.86610	0.36181	0.88459	0.10420	0.15696	1.57523	1.41827	0.70820	1.10935	0.40115
						0.38193	1.96406	1.58213	0.69707	1.09085	0.39377

Figure 8 displays the contours of γ and δ for the artificial samples, created from flood data, listed in Table 10, confirming that the MLEs of both parameters exist and are unique across all AML-based datasets. To examine MCMC convergence behavior, results for the representative sample $\mathcal{S}[1]$ are presented. As shown in Figure 9, the posterior distributions of γ and δ appear approximately symmetric, whereas those of $R(t)$ and $h(t)$ display negative and positive skewness, respectively. Furthermore, the statistics summarized in Table 12, derived from 30,000 posterior samples, support the estimation results in Table 11 and align closely with the convergence behavior depicted in Figure 9.

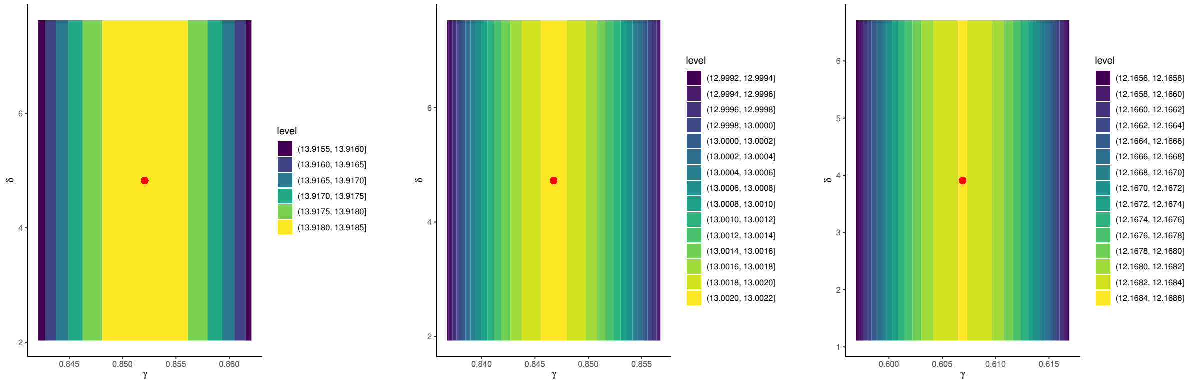

(a) $\mathcal{S}[1]$ (b) $\mathcal{S}[2]$ (c) $\mathcal{S}[3]$

Figure 8. Contours of γ (left) and δ (right) from flood data.

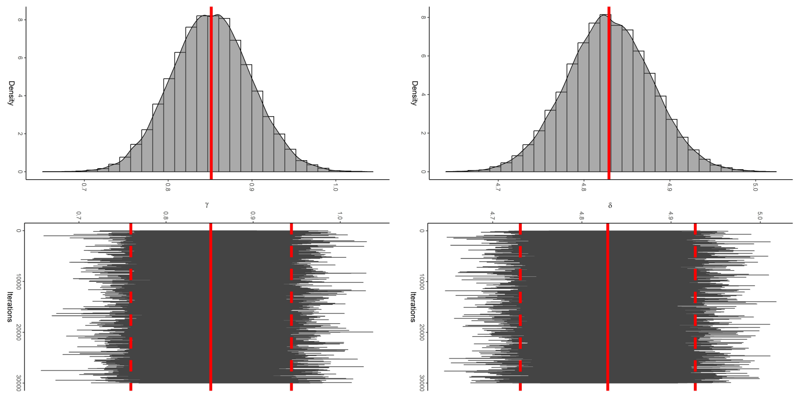

(a) δ (b) γ

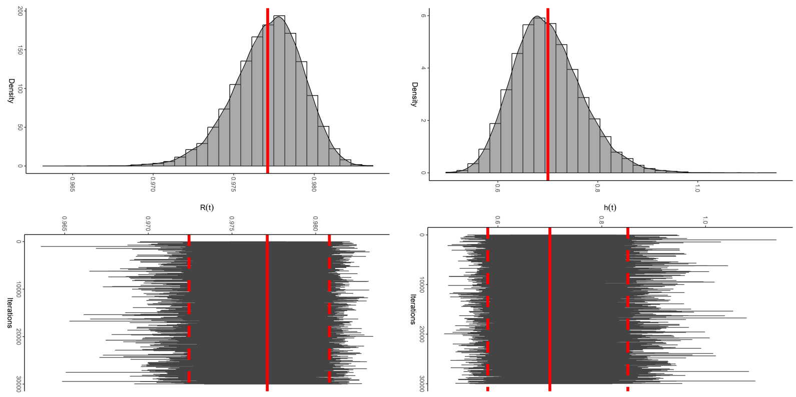

(c) $R(t)$ (d) $h(t)$

Figure 9. Density (left) and trace (right) plots of γ, δ, $R(t)$, and $h(t)$ from flood data.

Table 12. Summary for 30,000 MCMC iterations of γ, δ, $R(t)$, and $h(t)$ from flood data.

Sample	Par.	Mean	Mode	Q_1	Q_2	Q_3	Std.D	Skew.
$\mathcal{S}[1]$	γ	0.85135	0.82756	0.81942	0.85116	0.88296	0.04714	0.03195
	δ	4.82899	4.72651	4.79551	4.82857	4.86263	0.04987	0.00867
	$R(t)$	0.97711	0.97681	0.97578	0.97727	0.97861	0.00215	-0.49714
	$h(t)$	0.70011	0.70771	0.65175	0.69494	0.74283	0.06907	0.49207
$\mathcal{S}[2]$	γ	0.84571	0.84847	0.81377	0.84556	0.87724	0.04711	0.03159
	δ	4.72707	4.69488	4.69318	4.72695	4.76077	0.05006	0.02089
	$R(t)$	0.97745	0.97791	0.97614	0.97762	0.97891	0.00209	-0.46985
	$h(t)$	0.68735	0.67187	0.64039	0.68182	0.72907	0.06674	0.46372
$\mathcal{S}[3]$	γ	0.60216	0.59144	0.56968	0.60214	0.63407	0.04751	0.02943
	δ	3.91055	3.87426	3.87660	3.91052	3.94407	0.04994	0.02520
	$R(t)$	0.97042	0.97039	0.96832	0.97073	0.97281	0.00339	-0.54708
	$h(t)$	0.88459	0.85093	0.81201	0.87543	0.94845	0.10255	0.53179

6. Optimum censoring analysis

Determining the optimal T2-PC (i.e., the removal pattern design **R**) from the set of all feasible plans represents a significant challenge for practitioners in reliability analysis and life testing. This issue was first examined independently by Balakrishnan and Aggarwala [37] and Ng et al. [38], who explored several experimental configurations. The central objective of optimal progressive censoring is to identify, for fixed n and k, a censoring scheme $\mathbf{S} = (S_1, S_2, \ldots, S_k)$ that maximizes the information content about the unknown model parameters. In practice, the selection of an appropriate scheme depends on the experimenter's knowledge regarding the number of test units available, resource constraints, and associated testing costs.

Several studies have addressed the problem of identifying optimal censoring designs for various lifetime models; see, for instance, Pradhan and Kundu [39], Sen et al. [40], and Ashour et al. [41], among others. In this part, to select the optimal T2-PC plan, we consider three well-known criteria, namely:

- Criterion [A]: *Maximize* Trace$\{\mathbf{F}(\hat{\boldsymbol{\theta}})\}$, i.e., *Maximize*$\{-(\mathcal{L}_{11} + \mathcal{L}_{22})\}$;
- criterion [B]: *Minimize* Trace$\{\mathbf{F}^{-1}(\hat{\boldsymbol{\theta}})\}$, i.e., *Minimize*$\{\hat{\varepsilon}_{11} + \hat{\varepsilon}_{22}\}$;
- criterion [C]: *Minimize* Det$\{\mathbf{F}^{-1}(\hat{\boldsymbol{\theta}})\}$, i.e., *Minimize*$\{\hat{\varepsilon}_{11}\hat{\varepsilon}_{22} - \hat{\varepsilon}_{12}\hat{\varepsilon}_{21}\}$,

in such a way that, under criterion [A], the experimenter seeks to maximize the main diagonal elements of the observed FIM, $\mathbf{F}(\cdot)$, whereas under criteria [B] and [C], he aims to minimize the trace and determinant of the estimated VCM, $\mathbf{F}^{-1}(\cdot)$, respectively.

Using the generated T2-PC samples $\mathcal{S}[i]$ $(i = 1, 2, 3)$ derived from the carbon fiber and flood datasets presented in Tables 5 and 10, the corresponding optimal T2-PC censoring plans are determined and summarized in Table 13. The results indicate that:

- From carbon fiber data:
  - Using criterion [A], the left-censoring $(5^{[8]}, 0^{[21]})$ used in $\mathcal{S}[1]$ is the optimum censoring compared to others;
  - using criteria [B] and [C], the right-censoring $(0^{[21]}, 5^{[8]})$ used in $\mathcal{S}[3]$ is the optimum censoring compared to others.

- From flood data:
  - Using criteria [A], [B], and [C], the right-censoring ($0^{[10]}, 1^{[5]}$) used in $\mathcal{S}[3]$ is the optimum censoring compared to others.

Table 13. Optimum censoring from real datasets.

Sample↓ Criterion →	[A]	[B]	[C]
Carbon fiber data			
$\mathcal{S}[1]$	758.81	7.4841	0.0099
$\mathcal{S}[2]$	549.89	1.4231	0.0024
$\mathcal{S}[3]$	589.92	1.5201	0.0026
Flood data			
$\mathcal{S}[1]$	59.751	1.4905	0.0249
$\mathcal{S}[2]$	57.790	1.6227	0.0281
$\mathcal{S}[3]$	60.538	0.8429	0.0139

Table 13 further supports the conclusions drawn in the simulation study regarding the proposed censoring plans ($\mathcal{S}[i],\ i = 1, 2, 3$). In summary, the results confirm that the VFW lifetime model provides an appropriate and satisfactory description of the data under the proposed censoring schemes for both real-world datasets originating from engineering and physical sciences.

7. Conclusions

The present study investigates lifetime and reliability analysis by integrating the VFW distribution with the T2A-PC plan. The proposed framework effectively accommodates a wide range of hazard rate behaviors, including monotonic, unimodal, and two turning-point pattern (increase–decrease–increase) forms, while maintaining analytical tractability under complex censoring designs. This integration establishes a unified inferential scheme that enhances modeling flexibility, estimation accuracy, and experimental efficiency. Methodologically, new likelihood-based and Bayesian estimation procedures are developed, supported by asymptotic and credible interval constructions. Bayesian inference, implemented via the Metropolis–Hastings algorithm, yields stable, unbiased, and precise parameter estimates even under severe censoring conditions. Simulation analyses demonstrate that Bayesian estimators outperform their classical likelihood counterparts and that adaptive censoring substantially increases the effective information content of the sample. Moreover, comparative results confirm the superior performance of the VFW model relative to several well-known Weibull-type and generalized lifetime distributions in the literature. The VFW model consistently exhibits remarkable flexibility in capturing complex failure-time behaviors and achieves the best goodness-of-fit across both simulated and real engineering datasets. Collectively, these findings establish the VFW model, under the proposed adaptive censored sampling, as a robust and versatile tool for modern reliability studies. The proposed approach provides a flexible platform for constructing asymptotic and Bayesian interval estimates, supported by extensive simulation studies confirming the efficiency and reliability of the estimators. From a practical perspective, the adaptive censoring scheme allows experimenters to control test duration dynamically, manage sample utilization effectively, and accommodate complex censoring patterns often encountered in engineering and physical systems. Furthermore, the framework demonstrates strong applicability to real-world data, delivering accurate reliability and hazard function estimation for both engineering repairable systems and biomedical survival studies. Subsequently, the developed procedures provide reliability practitioners with efficient methods for experiment design and parameter estimation under progressive adaptive censoring. The demonstrated adaptability of the Bayesian framework further supports its adoption as a preferred inferential approach for lifetime data characterized by non-standard hazard rate patterns. Finally, this work opens avenues for future research, including the extension of adaptive progressive censoring designs to multivariate reliability models, optimal selection of censoring schemes, and integration with other flexible lifetime distributions to enhance predictive performance in diverse reliability contexts. Since the VFW model introduces only one additional parameter compared with the classical Weibull distribution, it may offer a reasonable compromise between model flexibility and parsimony in certain reliability investigations. Future research could extend the present work by conducting comparative studies with other alternative parametric, semi-parametric, or non-parametric approaches of varying complexity to further assess the practical performance of the proposed inference procedures in broader modeling frameworks. Moreover, extending the VFW model to incorporate covariates for assessing treatment effects or other survival-modifying factors under the proposed censoring scheme represents a promising direction for future research. Future research may also extend this work to hybrid and multivariate censoring schemes, accelerated life testing, and stress–strength reliability models to broaden the practical scope of the proposed methodology.

Author contributions

Ahmed Elshahhat: Writing–original draft, writing–review and editing, software; Osama E. Abo-Kasem: Methodology, writing–review and editing; Heba S. Mohammed: Methodology, funding acquisition, writing–review and editing. All authors have read and agreed to the published version of the manuscript.

Use of Generative-AI tools declaration

The authors declare they have not used Artificial Intelligence (AI) tools in the creation of this article.

Funding

This research was funded by the Princess Nourah bint Abdulrahman University Researchers Supporting Project number (PNURSP2026R175), Princess Nourah bint Abdulrahman University, Riyadh, Saudi Arabia.

Conflict of interest

There is no conflict of interest.

References

1. S. J. Almalki, J. Yuan, A new modified Weibull distribution, *Reliab. Eng. Syst. Saf.*, **111** (2013), 164–170. https://doi.org/10.1016/j.ress.2012.10.018
2. Z. Ahmad, Z. Hussain, Very flexible Weibull distribution, *MAYFEB J. Math.*, **2** (2017), 61–73. https://doi.org/10.22632/ccs-2017-252-30
3. E. S. Brito, P. H. Ferreira, V. L. Tomazella, D. S. M. Neto, R. S. Ehlers, Inference methods for the very flexible Weibull distribution based on progressive type-II censoring, *Commun. Stat.-Simul. C.*, **53** (2024), 5342–5366. https://doi.org/10.1080/03610918.2023.2180646
4. G. S. Mudholkar, D. K. Srivastava, Exponentiated Weibull family for analyzing bathtub failure-rate data, *IEEE T. Reliab.*, **42** (1993), 299–302. https://doi.org/10.1109/24.229504
5. M. Bebbington, C. D. Lai, R. Zitikis, A flexible Weibull extension, *Reliab. Eng. Syst. Saf.*, **92** (2007), 719–726. https://doi.org/10.1016/j.ress.2006.03.004
6. A. Elshahhat, E. A. Seyam, Very flexible Weibull reliability modeling for shock environments using unified censoring plans, *Mathematics*, **13** (2025), 3896. https://doi.org/10.3390/math13243896
7. J. D. Kalbfleisch, R. L. Prentice, *The statistical analysis of failure time data*, Wiley, 2002. https://doi.org/10.2307/2530581
8. J. F. Lawless, *Statistical models and methods for lifetime data*, Wiley, 2011. https://doi.org/10.1002/9781118033005
9. H. K. T. Ng, D. Kundu, P. S. Chan, Statistical analysis of exponential lifetimes under an adaptive type-II progressive censoring scheme, *Nav. Res. Log.*, **56** (2009), 687–698. https://doi.org/10.1002/nav.20371
10. S. Liu, W. Gui, Estimating parameters of the two-parameter Rayleigh distribution under adaptive progressive censoring with competing risks, *Mathematics*, **8** (2020), 1783. https://doi.org/10.3390/math8101783
11. A. Elshahhat, M. Nassar, Bayesian survival analysis for adaptive type-II progressive censored Hjorth data, *Computation. Stat.*, **36** (2021), 1965–1990. https://doi.org/10.1007/s00180-021-01065-8
12. S. Chen, W. Gui, Statistical analysis of a lifetime distribution with a bathtub-shaped failure rate function under adaptive progressive type-II censoring, *Mathematics*, **8** (2020), 670. https://doi.org/10.3390/math8050670
13. J. Kazempoor, A. Habibirad, A. A. Nadi, G. R. M. Borzadaran, Statistical inferences for the Weibull distribution under adaptive progressive type-II censoring plan and their application in wind speed data analysis, *Stat. Optim. Inf. Comput.*, **11** (2023), 829–852. https://doi.org/10.19139/soic-2310-5070-1501
14. Q. Lv, Y. Tian, W. Gui, Statistical inference for Gompertz distribution under adaptive progressive hybrid censoring, *J. Appl. Stat.*, **51** (2024), 451–480. https://doi.org/10.1080/02664763.2022.2136147

15. S. Dutta, S. Dey, S. Kayal, Bayesian survival analysis of logistic exponential distribution for adaptive progressive Type-II censored data, *Computation. Stat.*, **39** (2024), 2109–2155. https://doi.org/10.1007/s00180-023-01376-y

16. A. Kohansal, C. J. P. González, A. J. Fernández, Family of Kumaraswamy generalized distribution in estimation of multi-component reliability under the adaptive hybrid progressive censoring schemes, *Qual. Technol. Quant. M.*, **22** (2025), 280–320. https://doi.org/10.1080/16843703.2024.2315830

17. H. Sharma, P. Kumar, On survival estimation of Lomax distribution under adaptive progressive type-II censoring, *Stat. Tran. New Ser.*, **26** (2025), 51–67. https://doi.org/10.59139/stattrans-2025-004

18. A. Henningsen, O. Toomet, maxLik: A package for maximum likelihood estimation in R, *Computation. Stat.*, **26** (2011), 443–458. https://doi.org/10.32614/cran.package.maxlik

19. W. H. Greene, *Econometric analysis*, New Jersey: Pearson Prentice-Hall, 2012. https://doi.org/10.1007/s00362-010-0315-8

20. W. Q. Meeker, L. A. Escobar, *Statistical methods for reliability data*, New York: Wiley and Sons, 1998. https://doi.org/10.2307/1271181

21. D. Kundu, Bayesian inference and life testing plan for the Weibull distribution in presence of progressive censoring, *Technometrics*, **50** (2008), 144–154. https://doi.org/10.1198/004017008000000217

22. M. Plummer, N. Best, K. Cowles, K. Vines, CODA: Convergence diagnosis and output analysis for MCMC, *R News*, **6** (2006), 7–11. https://doi.org/10.32614/cran.package.coda

23. E. A. Ahmed, L. A. Al-Essa, Inference of stress-strength reliability based on adaptive progressive type-II censoring from Chen distribution with application to carbon fiber data, *AIMS Math.*, **9** (2024), 20482–20515. https://doi.org/10.3934/math.2024996

24. P. R. D. Marinho, R. B. Silva, M. Bourguignon, G. M. Cordeiro, S. Nadarajah, AdequacyModel: An R package for probability distributions and general purpose optimization, *PLoS One*, **14** (2019), e0221487. https://doi.org/10.1371/journal.pone.0221487

25. X. Peng, Z. Yan, Estimation and application for a new extended Weibull distribution, *Reliab. Eng. Syst. Saf.*, **121** (2014), 34–42. https://doi.org/10.1016/j.ress.2013.07.007

26. V. Bagdonavicius, M. Nikulin, *Accelerated life models: Modeling and statistical analysis*, Chapman and Hall/CRC, 2001. https://doi.org/10.1201/9781420035872

27. L. G. B. Pinho, G. M. Cordeiro, J. S. Nobre, The Harris extended exponential distribution, *Commun. Stat.-Theory M.*, **44** (2015), 3486–3502. https://doi.org/10.1080/03610926.2013.851221

28. R. Alotaibi, M. Nassar, A. Elshahhat, A new extended Pham distribution for modelling cancer data, *J. Radiat. Res. Appl. Sc.*, **17** (2024), 100961. https://doi.org/10.1016/j.jrras.2024.100961

29. P. E. Oguntunde, O. S. Balogun, H. I. Okagbue, S. A. Bishop, The Weibull-exponential distribution: Its properties and applications, *J. Appl. Sci.*, **15** (2015), 1305–1311. https://doi.org/10.3923/jas.2015.1305.1311

30. A. W. Marshall, I. Olkin, *Life distributions*, New York: Springer, 2007.

31. A. Mahdavi, D. Kundu, A new method for generating distributions with an application to exponential distribution, *Commun. Stat.-Theory M.*, **46** (2017), 6543–6557. https://doi.org/10.1080/03610926.2015.1130839
32. R. D. Gupta, D. Kundu, Generalized exponential distribution: Different method of estimations, *J. Stat. Comput. Sim.*, **69** (2001), 315–337. https://doi.org/10.1080/00949650108812098
33. Z. W. Birnbaum, S. C. Saunders, A probabilistic interpretation of Miner's rule, *SIAM J. Appl. Math.*, **16** (1968), 637–652. https://doi.org/10.1137/0116052
34. W. Weibull, A statistical distribution function of wide applicability, *J. Appl. Mech.*, **18** (1951), 293–297. https://doi.org/10.1115/1.4010337
35. N. Johnson, S. Kotz, N. Balakrishnan, *Continuous univariate distributions*, New York: Wiley, 1994. https://doi.org/10.2307/2291699
36. E. H. Khalifa, D. A. Ramadan, H. N. Alqifari, B. S. El-Desouky, Bayesian inference for inverse power exponentiated Pareto distribution using progressive type-II censoring with application to flood-level data analysis, *Symmetry*, **16** (2024), 309. https://doi.org/10.3390/sym16030309
37. N. Balakrishnan, R. Aggarwala, *Progressive censoring: Theory, methods, and applications*, Boston: Springer, 2000. https://doi.org/10.1007/978-1-4612-1334-5
38. H. K. T. Ng, P. S. Chan, N. Balakrishnan, Optimal progressive censoring plans for the Weibull distribution, *Technometrics*, **46** (2004), 470–481. https://doi.org/10.1198/004017004000000482
39. B. Pradhan, D. Kundu, Inference and optimal censoring schemes for progressively censored Birnbaum–Saunders distribution, *J. Stat. Plan. Infer.*, **143** (2013), 1098–1108. https://doi.org/10.1016/j.jspi.2012.11.007
40. T. Sen, Y. M. Tripathi, R. Bhattacharya, Statistical inference and optimum life testing plans under type-II hybrid censoring scheme, *Ann. Data Sci.*, **5** (2018), 679–708. https://doi.org/10.1007/s40745-018-0158-z
41. S. K. Ashour, A. A. El-Sheikh, A. Elshahhat, Inferences and optimal censoring schemes for progressively first-failure censored Nadarajah–Haghighi distribution, *Sankhya A*, **84** (2022), 885–923. https://doi.org/10.1007/s13171-019-00175-2

Appendix 1

This appendix provides all estimation outputs related to γ, δ, $R(t)$, and $h(t)$ derived from Monte Carlo simulations.

Table S1. The RMSEs (1st col.) and ARABs (2nd col.) of γ.

(n,k)		MLE		Bayes [Prior A]		Bayes [Prior B]		MLE		Bayes [Prior A]		Bayes [Prior B]	
Set 1 →				$T=0.5$						$T=1.5$			
(30,10)	[1]	1.0937	1.2037	0.8387	0.8582	0.5089	0.6869	1.0038	1.0630	0.6720	0.7073	0.4248	0.5672
	[2]	1.1266	1.3188	0.9111	0.9166	0.6953	0.7334	1.0337	1.1174	0.7291	0.7544	0.5615	0.6052
	[3]	1.0432	1.1485	0.8217	0.8542	0.4483	0.6059	0.9908	0.8573	0.6609	0.6863	0.3739	0.4916
(30,20)	[1]	0.9979	0.9637	0.6702	0.7822	0.3331	0.4956	0.8127	0.7993	0.5417	0.6265	0.2889	0.4035
	[2]	1.0012	0.9825	0.7395	0.8000	0.4244	0.5587	0.9862	0.8302	0.5932	0.6674	0.3676	0.4523
	[3]	0.9677	0.9600	0.6032	0.7613	0.3262	0.4373	0.8036	0.7873	0.5003	0.6135	0.2883	0.3772
(50,20)	[1]	0.8930	0.9488	0.5835	0.7602	0.2562	0.4141	0.8003	0.7808	0.4750	0.6113	0.2374	0.3735
	[2]	0.8776	0.9166	0.4422	0.7266	0.2006	0.4082	0.8000	0.7734	0.3763	0.5825	0.1911	0.3457
	[3]	0.8762	0.8227	0.3255	0.6399	0.1993	0.4039	0.7907	0.7640	0.2901	0.5164	0.1833	0.3311
(50,40)	[1]	0.7853	0.7163	0.2933	0.5514	0.1734	0.3839	0.7209	0.6663	0.2535	0.4461	0.1693	0.3243
	[2]	0.7958	0.8092	0.2933	0.5824	0.1993	0.3959	0.7899	0.7351	0.2535	0.4686	0.1833	0.3274
	[3]	0.7554	0.7021	0.2678	0.5476	0.1693	0.3666	0.7183	0.6024	0.2379	0.4425	0.1685	0.3223
(80,30)	[1]	0.7300	0.6720	0.2678	0.4735	0.1685	0.2425	0.6477	0.5678	0.2379	0.4092	0.1633	0.2208
	[2]	0.7290	0.6365	0.2654	0.4225	0.1685	0.2323	0.6375	0.5218	0.2320	0.3455	0.1633	0.1974
	[3]	0.4540	0.4871	0.2654	0.3654	0.1514	0.2206	0.3984	0.4828	0.2320	0.2951	0.1498	0.1973
(80,60)	[1]	0.3908	0.4805	0.1658	0.3145	0.1494	0.1929	0.3724	0.4341	0.1629	0.2609	0.1441	0.1745
	[2]	0.4140	0.4827	0.2295	0.3375	0.1514	0.2019	0.3984	0.4345	0.2262	0.2784	0.1498	0.1844
	[3]	0.3908	0.4785	0.1658	0.1438	0.1494	0.1250	0.3724	0.4100	0.1629	0.1430	0.1441	0.1216
Set 2 →				$T=0.5$						$T=1.5$			
(30,10)	[1]	2.1203	1.8000	1.1651	1.3107	0.8399	0.8312	1.5127	1.4968	0.9983	0.9994	0.6447	0.7277
	[2]	2.2494	1.8644	1.4541	1.4294	0.9097	0.9028	1.6375	1.6252	1.0151	0.9895	0.8074	0.7936
	[3]	2.0770	1.7989	1.0369	1.1525	0.8274	0.8301	1.4900	1.4952	0.9990	0.9982	0.5699	0.6372
(30,20)	[1]	1.8000	1.7483	0.9599	1.0638	0.7456	0.7605	1.3431	1.3698	0.9598	0.9588	0.5261	0.5895
	[2]	1.9368	1.7970	1.0314	1.0657	0.7689	0.8225	1.3853	1.4809	0.9965	0.9703	0.5664	0.5895
	[3]	1.7985	1.7313	0.9473	1.0177	0.6776	0.7157	1.2216	1.2891	0.8755	0.9417	0.4807	0.5561
(50,20)	[1]	1.7970	1.7309	0.9288	0.9226	0.5883	0.5775	1.0656	1.0423	0.6662	0.8940	0.3587	0.5102
	[2]	1.7362	1.6997	0.9108	0.7797	0.5356	0.4416	0.9732	0.7980	0.6118	0.7679	0.3305	0.4308
	[3]	1.6776	1.4359	0.8572	0.6938	0.4941	0.4295	0.8947	0.7879	0.5752	0.6215	0.3028	0.3820
(50,40)	[1]	1.6274	1.2001	0.7336	0.5845	0.4046	0.3552	0.7606	0.6458	0.5353	0.4696	0.2893	0.2449
	[2]	1.6575	1.3610	0.7708	0.6115	0.4211	0.3645	0.8253	0.6619	0.5353	0.4721	0.2893	0.2537
	[3]	1.5108	1.1713	0.7336	0.5500	0.4046	0.3025	0.7415	0.5561	0.4647	0.4223	0.2386	0.2272
(80,30)	[1]	1.4558	1.0373	0.5812	0.5120	0.3375	0.2967	0.6208	0.5460	0.4031	0.3749	0.2060	0.1928
	[2]	1.3843	0.9605	0.5620	0.4175	0.3051	0.2133	0.5750	0.4943	0.3902	0.2789	0.2018	0.1314
	[3]	0.8249	0.9489	0.4298	0.3463	0.3051	0.1610	0.5620	0.4384	0.3902	0.2379	0.2018	0.1056
(80,60)	[1]	0.8093	0.9197	0.2961	0.2647	0.1438	0.1181	0.4080	0.4350	0.2237	0.2071	0.1016	0.0918
	[2]	0.8249	0.9222	0.4298	0.2789	0.2134	0.1350	0.4393	0.4382	0.2676	0.2211	0.1203	0.1006
	[3]	0.8087	0.7944	0.2961	0.2085	0.1438	0.0954	0.4078	0.4081	0.2237	0.1616	0.1016	0.0714

Table S2. The RMSEs (1st col.) and ARABs (2nd col.) of δ.

(n, k)		MLE		Bayes [Prior A]		Bayes [Prior B]		MLE		Bayes [Prior A]		Bayes [Prior B]	
Set 1 →				$T = 0.5$						$T = 1.5$			
(30,10)	[1]	2.7076	3.9075	2.2098	3.1079	1.2736	1.8218	2.3492	3.5533	1.5940	2.1153	0.8949	1.6441
	[2]	2.6224	3.6920	1.4520	2.8161	1.1994	1.5445	2.0974	3.3609	1.2660	1.9683	0.5185	1.3386
	[3]	2.6718	3.7799	1.8063	2.9150	1.2062	1.7688	2.1390	3.2164	1.5044	1.9889	0.7448	1.5696
(30,20)	[1]	2.5412	3.2081	1.2407	2.6939	0.7556	1.4727	1.8705	2.8075	0.9063	1.7985	0.3927	1.0882
	[2]	2.4824	3.1904	1.1326	2.6874	0.7313	1.3994	1.7617	2.6325	0.8814	1.6844	0.3538	1.0819
	[3]	2.5875	3.4862	1.3783	2.7801	0.7811	1.5366	1.9485	3.1096	1.1086	1.9177	0.5011	1.2700
(50,20)	[1]	2.4330	3.0650	1.0413	1.6806	0.5853	1.3070	1.3517	2.5455	0.8381	1.6792	0.3258	0.6771
	[2]	2.0336	2.8238	0.8407	1.6253	0.4853	1.0633	1.2947	2.2745	0.6436	1.4973	0.2947	0.6447
	[3]	2.3880	3.0507	0.9755	1.6803	0.5253	1.2514	1.3517	2.3287	0.6630	1.6279	0.2999	0.6748
(50,40)	[1]	1.6921	2.4538	0.8083	1.1838	0.3847	0.8054	0.9047	2.0120	0.6092	1.0521	0.2608	0.5077
	[2]	1.6739	2.2267	0.6990	1.1623	0.3702	0.7842	0.9047	1.9464	0.4573	0.9830	0.2143	0.4823
	[3]	1.7574	2.6090	0.8165	1.2574	0.4205	0.8852	1.0168	2.2111	0.6092	1.1323	0.2608	0.5250
(80,30)	[1]	0.9731	2.2147	0.4550	1.1569	0.3702	0.7141	0.8891	1.7753	0.4436	0.9091	0.2058	0.4798
	[2]	0.7325	2.0230	0.4409	0.9702	0.2727	0.5347	0.6281	1.3249	0.3397	0.8894	0.2010	0.4382
	[3]	0.9548	2.1428	0.4441	1.1063	0.2727	0.6227	0.6281	1.5535	0.4409	0.8932	0.2010	0.4667
(80,60)	[1]	0.7153	1.6695	0.3358	0.7168	0.1712	0.4702	0.3760	1.1636	0.2297	0.6300	0.1128	0.2684
	[2]	0.7083	1.4132	0.3358	0.6758	0.1712	0.3875	0.3760	0.9533	0.2297	0.5789	0.1128	0.2578
	[3]	0.7325	1.7779	0.3397	0.8132	0.2600	0.5020	0.5492	1.2340	0.3199	0.6743	0.1579	0.2879
Set 2 →				$T = 0.5$						$T = 1.5$			
(30,10)	[1]	1.0597	2.9150	0.8078	2.0302	0.6673	1.5616	0.9343	2.1901	0.7483	1.6543	0.5758	1.4482
	[2]	1.0253	2.4316	0.7637	1.9630	0.6550	1.4731	0.9180	2.1279	0.7062	1.5183	0.5440	1.3984
	[3]	1.1831	3.1371	0.8739	2.0378	0.6791	1.6380	0.9516	2.2971	0.7752	1.9228	0.6238	1.4525
(30,20)	[1]	0.9625	1.3490	0.6890	1.1597	0.6419	0.9616	0.8989	1.2350	0.6839	1.1184	0.4905	0.7958
	[2]	0.7993	1.0125	0.6230	0.9801	0.5549	0.7204	0.7776	1.0090	0.5627	0.7698	0.4341	0.6995
	[3]	0.9118	1.2342	0.6466	1.0652	0.6129	0.7911	0.8586	1.0958	0.6321	0.8812	0.4438	0.7581
(50,20)	[1]	0.7002	0.9543	0.5166	0.8741	0.3996	0.6532	0.5596	0.9187	0.4884	0.6815	0.3672	0.6236
	[2]	0.6974	0.9498	0.4879	0.7593	0.3970	0.6327	0.5574	0.9067	0.4829	0.6778	0.3479	0.5420
	[3]	0.7725	0.9745	0.5364	0.9419	0.4526	0.6956	0.6340	0.9438	0.5234	0.7124	0.3733	0.6739
(50,40)	[1]	0.5245	0.8934	0.4879	0.6529	0.3543	0.5856	0.5052	0.8200	0.3744	0.6225	0.3479	0.4618
	[2]	0.4664	0.8205	0.4136	0.5792	0.2920	0.4348	0.4600	0.6092	0.3319	0.5687	0.2884	0.4053
	[3]	0.5245	0.8771	0.4520	0.6488	0.3181	0.5419	0.4641	0.7589	0.3437	0.6170	0.2916	0.4572
(80,30)	[1]	0.4537	0.4050	0.3578	0.2901	0.2622	0.2256	0.3780	0.3163	0.3228	0.2805	0.2524	0.2063
	[2]	0.3413	0.3993	0.2632	0.1910	0.2071	0.1348	0.3164	0.2695	0.2387	0.1586	0.1792	0.1041
	[3]	0.4664	0.5483	0.4006	0.4175	0.2920	0.3373	0.4136	0.4736	0.3319	0.3737	0.2831	0.2951
(80,60)	[1]	0.3164	0.3489	0.2071	0.1851	0.1226	0.1275	0.2358	0.2297	0.1659	0.1484	0.0773	0.1010
	[2]	0.3103	0.2415	0.0760	0.0591	0.0473	0.0334	0.2021	0.1489	0.0584	0.0472	0.0332	0.0271
	[3]	0.3131	0.2728	0.0760	0.0810	0.0493	0.0512	0.2021	0.1809	0.0584	0.0680	0.0332	0.0412

Table S3. The RMSEs (1st col.) and ARABs (2nd col.) of $R(t)$.

(n,k)		MLE		Bayes [Prior A]		Bayes [Prior B]		MLE		Bayes [Prior A]		Bayes [Prior B]	
Set 1 →				$T = 0.5$						$T = 1.5$			
(30,10)	[1]	0.2272	0.2216	0.1882	0.1748	0.1316	0.1341	0.2079	0.1848	0.1588	0.1519	0.1136	0.1324
	[2]	0.1997	0.1931	0.1751	0.1591	0.1108	0.1188	0.1835	0.1653	0.1483	0.1477	0.0999	0.1166
	[3]	0.2109	0.2065	0.1788	0.1647	0.1265	0.1265	0.1973	0.1695	0.1452	0.1494	0.1054	0.1246
(30,20)	[1]	0.1875	0.1740	0.1613	0.1522	0.0612	0.1116	0.1732	0.1613	0.1439	0.1431	0.0554	0.1097
	[2]	0.1873	0.1696	0.1570	0.1506	0.0596	0.1016	0.1710	0.1572	0.1433	0.1410	0.0475	0.1011
	[3]	0.1939	0.1771	0.1650	0.1548	0.1003	0.1142	0.1782	0.1635	0.1468	0.1445	0.0804	0.1131
(50,20)	[1]	0.1833	0.1695	0.1548	0.1492	0.0536	0.0943	0.1704	0.1562	0.1415	0.1375	0.0456	0.0808
	[2]	0.1783	0.1635	0.1473	0.1433	0.0348	0.0518	0.1669	0.1506	0.1381	0.1303	0.0324	0.0515
	[3]	0.1808	0.1675	0.1496	0.1458	0.0488	0.0582	0.1689	0.1549	0.1399	0.1365	0.0454	0.0581
(50,40)	[1]	0.1737	0.1618	0.1406	0.1401	0.0275	0.0432	0.1617	0.1419	0.1351	0.1254	0.0242	0.0396
	[2]	0.1720	0.1602	0.1403	0.1290	0.0264	0.0368	0.1604	0.1406	0.1342	0.1174	0.0224	0.0342
	[3]	0.1745	0.1633	0.1434	0.1413	0.0291	0.0490	0.1635	0.1450	0.1366	0.1291	0.0269	0.0435
(80,30)	[1]	0.1692	0.1557	0.1344	0.1164	0.0215	0.0326	0.1519	0.1372	0.1284	0.1081	0.0211	0.0323
	[2]	0.1605	0.1437	0.1314	0.1096	0.0190	0.0210	0.1481	0.1281	0.1234	0.1034	0.0182	0.0207
	[3]	0.1646	0.1488	0.1334	0.1123	0.0200	0.0258	0.1507	0.1320	0.1261	0.1050	0.0190	0.0257
(80,60)	[1]	0.1555	0.1212	0.1269	0.0897	0.0152	0.0140	0.1371	0.1114	0.1170	0.0895	0.0143	0.0135
	[2]	0.1414	0.1175	0.1199	0.0819	0.0126	0.0131	0.1264	0.1088	0.1071	0.0782	0.0110	0.0116
	[3]	0.1584	0.1384	0.1282	0.0948	0.0170	0.0153	0.1440	0.1243	0.1210	0.0928	0.0163	0.0150
Set 2 →				$T = 0.5$						$T = 1.5$			
(30,10)	[1]	0.2076	0.1873	0.1569	0.1524	0.1198	0.1239	0.1594	0.1574	0.1404	0.1408	0.0932	0.0373
	[2]	0.1976	0.1832	0.1488	0.1437	0.1072	0.1158	0.1508	0.1459	0.1362	0.1316	0.0908	0.0372
	[3]	0.2176	0.1952	0.1673	0.1660	0.1279	0.1329	0.1735	0.1664	0.1549	0.1511	0.1008	0.0456
(30,20)	[1]	0.1671	0.1802	0.1139	0.1355	0.0870	0.1090	0.1379	0.1369	0.1127	0.1238	0.0779	0.0361
	[2]	0.1278	0.1554	0.0933	0.1146	0.0767	0.0932	0.0983	0.1184	0.0871	0.1059	0.0639	0.0350
	[3]	0.1401	0.1772	0.1015	0.1326	0.0841	0.1063	0.1086	0.1333	0.0955	0.1208	0.0700	0.0357
(50,20)	[1]	0.1033	0.0761	0.0706	0.0529	0.0620	0.0457	0.0843	0.0613	0.0704	0.0519	0.0516	0.0334
	[2]	0.0847	0.0543	0.0614	0.0375	0.0508	0.0333	0.0656	0.0439	0.0577	0.0370	0.0423	0.0326
	[3]	0.1142	0.0922	0.0808	0.0629	0.0685	0.0553	0.0905	0.0803	0.0779	0.0580	0.0571	0.0347
(50,40)	[1]	0.0615	0.0466	0.0440	0.0323	0.0369	0.0284	0.0483	0.0376	0.0419	0.0318	0.0308	0.0280
	[2]	0.0534	0.0371	0.0370	0.0267	0.0320	0.0223	0.0431	0.0290	0.0364	0.0253	0.0267	0.0219
	[3]	0.0584	0.0418	0.0418	0.0308	0.0350	0.0251	0.0458	0.0318	0.0398	0.0285	0.0292	0.0247
(80,30)	[1]	0.0339	0.0279	0.0256	0.0204	0.0203	0.0167	0.0272	0.0214	0.0231	0.0190	0.0179	0.0133
	[2]	0.0338	0.0236	0.0231	0.0173	0.0203	0.0141	0.0253	0.0180	0.0223	0.0161	0.0169	0.0121
	[3]	0.0378	0.0327	0.0285	0.0242	0.0227	0.0196	0.0295	0.0249	0.0257	0.0223	0.0189	0.0159
(80,60)	[1]	0.0280	0.0180	0.0208	0.0131	0.0168	0.0115	0.0213	0.0139	0.0191	0.0123	0.0140	0.0108
	[2]	0.0154	0.0121	0.0108	0.0090	0.0092	0.0080	0.0123	0.0109	0.0135	0.0101	0.0077	0.0073
	[3]	0.0241	0.0160	0.0173	0.0111	0.0145	0.0096	0.0189	0.0130	0.0165	0.0109	0.0121	0.0088

Table S4. The RMSEs (1st col.) and ARABs (2nd col.) of $h(t)$.

(n,k)		MLE		Bayes [Prior A]		Bayes [Prior B]		MLE		Bayes [Prior A]		Bayes [Prior B]	
Set 1 →				$T=0.5$						$T=1.5$			
(30,10)	[1]	2.9350	2.1827	2.0814	1.9546	0.8467	0.7713	2.1476	2.0201	1.5520	1.8678	0.8373	0.7201
	[2]	3.1413	2.3239	2.1931	1.9776	0.8774	0.7848	2.2249	2.2363	1.6482	1.9275	0.8671	0.7556
	[3]	3.2350	2.4612	2.2486	2.1293	0.9125	0.7983	2.4692	2.3206	1.8731	2.0010	0.8906	0.7947
(30,20)	[1]	2.5135	1.9941	1.9440	1.8140	0.8062	0.7550	1.9966	1.9269	1.0396	1.7673	0.7763	0.6884
	[2]	2.8313	2.1480	1.9814	1.9461	0.8351	0.7665	2.0473	1.9655	1.5061	1.8532	0.8074	0.7118
	[3]	2.7473	2.0328	1.9746	1.8940	0.8235	0.7587	2.0097	1.9331	1.0508	1.7819	0.7833	0.6920
(50,20)	[1]	1.9770	1.8537	1.6286	1.6329	0.7690	0.7107	1.8906	1.7078	0.7847	0.9728	0.5837	0.5769
	[2]	2.0267	1.9037	1.9219	1.7347	0.7738	0.7341	1.9655	1.8034	0.8144	1.1060	0.7526	0.6141
	[3]	2.1606	1.9148	1.9399	1.7534	0.7903	0.7531	1.9866	1.9237	0.9135	1.5748	0.7629	0.6487
(50,40)	[1]	1.9635	1.7190	1.1729	1.4266	0.7101	0.6411	1.8503	1.5245	0.7684	0.6821	0.4480	0.4458
	[2]	1.9755	1.8406	1.3405	1.6137	0.7338	0.7041	1.8625	1.6157	0.7847	0.9357	0.5060	0.5682
	[3]	1.9741	1.8259	1.2079	1.4957	0.7172	0.6937	1.8619	1.5828	0.7829	0.7308	0.4778	0.4926
(80,30)	[1]	1.8666	1.3105	0.7187	1.0557	0.2919	0.3743	1.6588	1.2129	0.5948	0.5471	0.1431	0.3303
	[2]	1.9252	1.3986	0.7545	1.2156	0.4233	0.4569	1.6893	1.3052	0.6134	0.5657	0.1869	0.3508
	[3]	1.9577	1.5873	0.7770	1.2678	0.4327	0.5600	1.7061	1.4281	0.6221	0.6238	0.2055	0.3558
(80,60)	[1]	1.5741	1.0511	0.5408	0.6264	0.2804	0.3108	1.2152	0.9263	0.2923	0.3521	0.1249	0.2385
	[2]	1.8649	1.2817	0.7184	0.7071	0.2919	0.3265	1.2845	1.0509	0.3534	0.5075	0.1306	0.2750
	[3]	1.7462	1.1075	0.6457	0.6547	0.2841	0.3149	1.2660	1.0029	0.3500	0.3708	0.1249	0.2552
Set 2 →				$T=0.5$						$T=1.5$			
(30,10)	[1]	2.5070	2.1525	1.3211	1.3365	0.6629	0.5482	2.4879	1.6813	0.8599	0.8700	0.2902	0.4741
	[2]	2.6630	2.2861	1.5822	1.4917	1.0345	0.7428	2.6241	1.9600	1.1810	0.9764	0.2954	0.4857
	[3]	2.8372	2.4271	1.8481	1.8133	1.3408	0.9304	2.7346	2.1019	1.5816	1.1744	0.7705	0.6088
(30,20)	[1]	1.9945	1.8901	0.3998	1.0463	0.2856	0.4389	1.6799	1.3098	0.3565	0.6845	0.2786	0.3245
	[2]	2.2244	2.1111	1.0103	1.2332	0.4058	0.4629	2.0996	1.4936	0.6654	0.8656	0.2863	0.4353
	[3]	2.1709	1.9555	0.4730	1.1305	0.3161	0.4418	1.9254	1.4565	0.3998	0.7366	0.2853	0.3692
(50,20)	[1]	1.3475	0.9358	0.3368	0.4418	0.2483	0.3113	1.1331	0.6516	0.3109	0.3773	0.2319	0.3096
	[2]	1.4482	1.0523	0.3864	0.4860	0.2483	0.3389	1.3714	0.6800	0.3322	0.4252	0.2462	0.3116
	[3]	1.7084	1.6607	0.3938	0.7584	0.2761	0.4265	1.6581	0.8756	0.3565	0.4958	0.2595	0.3210
(50,40)	[1]	0.8041	0.5170	0.2940	0.3784	0.1903	0.2738	0.7494	0.4693	0.2220	0.3612	0.1762	0.2684
	[2]	1.2542	0.8005	0.3138	0.4092	0.2369	0.3015	0.8593	0.5785	0.3063	0.3714	0.2311	0.2923
	[3]	1.0539	0.5718	0.3120	0.3831	0.2362	0.2755	0.8489	0.5111	0.2940	0.3653	0.2220	0.2721
(80,30)	[1]	0.4760	0.3134	0.1926	0.2790	0.1744	0.2485	0.2092	0.2964	0.1793	0.2590	0.1552	0.2328
	[2]	0.6450	0.3645	0.2460	0.2838	0.1855	0.2621	0.2845	0.3349	0.1958	0.2690	0.1588	0.2617
	[3]	0.7229	0.4412	0.2779	0.3558	0.1903	0.2731	0.3521	0.3699	0.2152	0.2873	0.1623	0.2644
(80,60)	[1]	0.4350	0.2243	0.1424	0.1659	0.1079	0.1404	0.1668	0.1873	0.1422	0.1415	0.1075	0.0929
	[2]	0.4760	0.2851	0.1774	0.2329	0.1462	0.2089	0.1926	0.2785	0.1652	0.2229	0.1407	0.2020
	[3]	0.4358	0.2773	0.1548	0.2123	0.1396	0.1855	0.1871	0.2330	0.1527	0.1987	0.1303	0.1049

Table S5. The AILs (1st col.) and CPs (2nd col.) of γ.

(n,k)		ACI-NA		ACI-NL		BCI [Prior A]		BCI [Prior B]		HPD [Prior A]		HPD [Prior B]	
Set 1 (for T = 0.5)													
(30,10)	[1]	2.038	0.912	2.547	0.897	0.853	0.947	0.792	0.949	0.597	0.955	0.572	0.956
	[2]	2.071	0.911	2.896	0.887	1.193	0.937	0.853	0.947	0.837	0.948	0.597	0.955
	[3]	1.804	0.919	2.255	0.906	0.843	0.948	0.573	0.955	0.544	0.956	0.531	0.957
(30,20)	[1]	1.318	0.934	1.647	0.924	0.693	0.952	0.564	0.956	0.508	0.957	0.498	0.958
	[2]	1.578	0.926	1.973	0.914	0.693	0.952	0.573	0.955	0.520	0.957	0.506	0.957
	[3]	1.178	0.938	1.546	0.927	0.670	0.953	0.559	0.956	0.501	0.958	0.481	0.958
(50,20)	[1]	1.158	0.938	1.478	0.929	0.626	0.954	0.534	0.957	0.492	0.958	0.419	0.960
	[2]	1.115	0.940	1.423	0.930	0.600	0.955	0.514	0.957	0.492	0.958	0.380	0.961
	[3]	1.115	0.940	1.399	0.931	0.589	0.955	0.494	0.958	0.488	0.958	0.376	0.961
(50,40)	[1]	0.813	0.948	1.308	0.934	0.545	0.956	0.484	0.958	0.437	0.959	0.324	0.963
	[2]	1.073	0.941	1.341	0.933	0.545	0.956	0.484	0.958	0.460	0.959	0.358	0.962
	[3]	0.813	0.948	1.308	0.934	0.506	0.957	0.480	0.958	0.432	0.960	0.323	0.963
(80,30)	[1]	0.700	0.952	1.197	0.937	0.473	0.958	0.435	0.960	0.420	0.960	0.319	0.963
	[2]	0.661	0.953	1.165	0.938	0.456	0.959	0.410	0.960	0.391	0.961	0.277	0.964
	[3]	0.520	0.957	1.045	0.942	0.437	0.959	0.376	0.961	0.328	0.963	0.230	0.966
(80,60)	[1]	0.397	0.961	0.894	0.946	0.365	0.962	0.337	0.962	0.236	0.965	0.154	0.968
	[2]	0.492	0.958	0.894	0.946	0.397	0.961	0.366	0.962	0.307	0.963	0.200	0.966
	[3]	0.387	0.961	0.715	0.951	0.350	0.962	0.155	0.968	0.139	0.968	0.127	0.969
Set 1 (for T = 1.5)													
(30,10)	[1]	1.397	0.931	2.052	0.912	0.837	0.948	0.770	0.950	0.589	0.955	0.562	0.956
	[2]	1.674	0.923	2.317	0.904	1.170	0.938	0.839	0.948	0.827	0.948	0.589	0.955
	[3]	1.071	0.941	2.022	0.913	0.825	0.948	0.565	0.956	0.535	0.957	0.525	0.957
(30,20)	[1]	0.718	0.951	1.319	0.933	0.675	0.952	0.557	0.956	0.499	0.958	0.482	0.958
	[2]	0.873	0.947	1.806	0.919	0.675	0.952	0.565	0.956	0.515	0.957	0.505	0.957
	[3]	0.684	0.952	1.236	0.936	0.655	0.953	0.549	0.956	0.493	0.958	0.481	0.958
(50,20)	[1]	0.640	0.954	1.183	0.938	0.615	0.954	0.516	0.957	0.480	0.958	0.413	0.960
	[2]	0.617	0.954	1.138	0.939	0.589	0.955	0.505	0.958	0.479	0.958	0.366	0.962
	[3]	0.600	0.955	1.119	0.939	0.534	0.957	0.491	0.958	0.479	0.958	0.352	0.962
(50,40)	[1]	0.552	0.956	0.957	0.944	0.490	0.958	0.463	0.959	0.425	0.960	0.317	0.963
	[2]	0.552	0.956	1.101	0.940	0.492	0.958	0.468	0.959	0.443	0.959	0.350	0.962
	[3]	0.531	0.957	0.932	0.945	0.490	0.958	0.461	0.959	0.422	0.960	0.304	0.963
(80,30)	[1]	0.482	0.958	0.836	0.948	0.458	0.959	0.422	0.960	0.407	0.960	0.295	0.964
	[2]	0.468	0.959	0.668	0.953	0.414	0.960	0.396	0.961	0.352	0.962	0.266	0.965
	[3]	0.458	0.959	0.618	0.954	0.389	0.961	0.331	0.963	0.303	0.963	0.219	0.966
(80,60)	[1]	0.375	0.961	0.401	0.961	0.362	0.962	0.257	0.965	0.175	0.967	0.150	0.968
	[2]	0.401	0.961	0.611	0.954	0.383	0.961	0.311	0.963	0.291	0.964	0.184	0.967
	[3]	0.356	0.962	0.393	0.961	0.276	0.964	0.142	0.968	0.139	0.968	0.115	0.969
Set 2 (for T = 0.5)													
(30,10)	[1]	2.287	0.909	2.600	0.894	1.745	0.943	1.526	0.945	1.204	0.950	1.121	0.951
	[2]	2.414	0.908	2.957	0.884	1.864	0.933	1.720	0.943	1.279	0.943	1.202	0.950
	[3]	2.175	0.915	2.297	0.902	1.700	0.943	1.526	0.951	1.196	0.952	1.121	0.952
(30,20)	[1]	1.877	0.929	2.101	0.920	1.627	0.947	1.160	0.951	1.109	0.953	0.987	0.953
	[2]	1.935	0.922	2.198	0.911	1.666	0.947	1.190	0.951	1.156	0.952	0.990	0.953
	[3]	1.716	0.933	2.053	0.923	1.411	0.948	1.160	0.951	1.037	0.953	0.966	0.953
(50,20)	[1]	1.670	0.934	1.711	0.925	1.175	0.949	1.114	0.952	0.958	0.953	0.918	0.955
	[2]	1.412	0.935	1.597	0.926	1.006	0.950	0.972	0.953	0.918	0.953	0.834	0.956
	[3]	1.237	0.935	1.413	0.927	0.941	0.950	0.924	0.953	0.862	0.953	0.831	0.956
(50,40)	[1]	1.159	0.944	1.316	0.930	0.907	0.952	0.833	0.953	0.745	0.955	0.667	0.958
	[2]	1.237	0.936	1.354	0.929	0.928	0.952	0.897	0.953	0.851	0.954	0.810	0.957
	[3]	0.987	0.944	1.316	0.930	0.844	0.953	0.829	0.953	0.700	0.955	0.652	0.958
(80,30)	[1]	0.983	0.947	1.305	0.933	0.806	0.954	0.644	0.955	0.598	0.955	0.469	0.958
	[2]	0.924	0.948	1.224	0.934	0.759	0.954	0.596	0.956	0.485	0.956	0.445	0.959
	[3]	0.860	0.952	1.161	0.937	0.726	0.955	0.574	0.956	0.472	0.958	0.413	0.961
(80,60)	[1]	0.646	0.956	0.911	0.942	0.559	0.957	0.446	0.958	0.353	0.960	0.303	0.963
	[2]	0.656	0.953	1.063	0.942	0.628	0.956	0.518	0.957	0.396	0.958	0.352	0.962
	[3]	0.454	0.956	0.636	0.947	0.387	0.957	0.308	0.963	0.197	0.963	0.183	0.964
Set 2 (for T = 1.5)													
(30,10)	[1]	2.227	0.927	2.394	0.908	1.697	0.943	1.488	0.945	1.187	0.950	1.104	0.951
	[2]	2.269	0.919	2.671	0.901	1.832	0.934	1.666	0.943	1.263	0.944	1.182	0.950
	[3]	2.057	0.936	2.216	0.909	1.666	0.944	1.488	0.951	1.177	0.952	1.104	0.952
(30,20)	[1]	1.717	0.947	1.888	0.929	1.601	0.948	1.139	0.951	1.095	0.953	0.969	0.953
	[2]	1.913	0.942	2.149	0.915	1.630	0.948	1.167	0.951	1.151	0.952	0.974	0.953
	[3]	1.708	0.948	1.725	0.932	1.383	0.948	1.139	0.951	1.022	0.953	0.948	0.953
(50,20)	[1]	1.539	0.949	1.700	0.933	1.148	0.950	1.081	0.952	0.944	0.953	0.905	0.955
	[2]	1.329	0.950	1.593	0.935	0.989	0.950	0.970	0.953	0.905	0.954	0.823	0.957
	[3]	1.212	0.950	1.385	0.935	0.928	0.952	0.907	0.953	0.847	0.954	0.805	0.957
(50,40)	[1]	1.084	0.951	1.281	0.940	0.882	0.953	0.817	0.954	0.733	0.955	0.644	0.958
	[2]	1.189	0.951	1.323	0.936	0.907	0.953	0.884	0.954	0.837	0.955	0.799	0.957
	[3]	0.873	0.952	1.180	0.940	0.830	0.953	0.817	0.954	0.685	0.955	0.642	0.959
(80,30)	[1]	0.829	0.953	1.154	0.943	0.799	0.954	0.625	0.955	0.580	0.956	0.459	0.959
	[2]	0.780	0.954	1.082	0.948	0.744	0.955	0.585	0.956	0.465	0.957	0.432	0.960
	[3]	0.743	0.954	1.078	0.950	0.581	0.956	0.573	0.958	0.457	0.959	0.391	0.961
(80,60)	[1]	0.628	0.956	0.863	0.956	0.476	0.957	0.428	0.960	0.340	0.962	0.284	0.963
	[2]	0.653	0.956	0.982	0.950	0.531	0.956	0.494	0.958	0.375	0.959	0.339	0.962
	[3]	0.441	0.957	0.474	0.956	0.371	0.959	0.278	0.963	0.188	0.963	0.174	0.964

Table S6. The AILs (1st col.) and CPs (2nd col.) of δ.

(n,k)		ACI-NA		ACI-NL		BCI [Prior A]		BCI [Prior B]		HPD [Prior A]		HPD [Prior B]	
Set 1 (for T = 0.5)													
(30,10)	[1]	1.601	0.924	1.396	0.931	1.228	0.937	1.121	0.941	1.098	0.942	0.976	0.947
	[2]	1.362	0.933	1.084	0.943	1.058	0.944	1.042	0.944	0.796	0.953	0.765	0.954
	[3]	1.457	0.929	1.294	0.935	1.125	0.941	1.090	0.942	0.994	0.946	0.895	0.949
(30,20)	[1]	1.275	0.936	0.940	0.948	0.873	0.950	0.755	0.954	0.750	0.955	0.544	0.962
	[2]	1.225	0.938	0.937	0.948	0.781	0.954	0.741	0.955	0.734	0.955	0.525	0.963
	[3]	1.306	0.935	1.018	0.945	1.002	0.946	0.804	0.953	0.780	0.954	0.557	0.962
(50,20)	[1]	1.146	0.940	0.889	0.950	0.747	0.955	0.724	0.956	0.652	0.958	0.513	0.963
	[2]	1.027	0.945	0.698	0.957	0.668	0.958	0.659	0.958	0.636	0.959	0.490	0.964
	[3]	1.054	0.944	0.834	0.952	0.694	0.957	0.670	0.958	0.649	0.958	0.503	0.964
(50,40)	[1]	0.995	0.946	0.623	0.959	0.620	0.959	0.613	0.960	0.575	0.961	0.406	0.967
	[2]	0.984	0.946	0.623	0.959	0.613	0.960	0.584	0.961	0.568	0.961	0.401	0.967
	[3]	1.027	0.945	0.643	0.959	0.633	0.959	0.628	0.959	0.622	0.959	0.409	0.967
(80,30)	[1]	0.942	0.948	0.584	0.961	0.558	0.962	0.551	0.962	0.542	0.962	0.391	0.968
	[2]	0.762	0.954	0.534	0.962	0.490	0.964	0.477	0.965	0.469	0.965	0.385	0.968
	[3]	0.856	0.951	0.542	0.962	0.501	0.964	0.497	0.964	0.494	0.964	0.390	0.968
(80,60)	[1]	0.608	0.960	0.521	0.963	0.479	0.964	0.454	0.965	0.354	0.969	0.295	0.971
	[2]	0.542	0.962	0.514	0.963	0.457	0.965	0.424	0.966	0.303	0.971	0.271	0.972
	[3]	0.726	0.956	0.526	0.963	0.481	0.964	0.469	0.965	0.457	0.965	0.378	0.968
Set 1 (for T = 1.5)													
(30,10)	[1]	1.297	0.935	1.319	0.934	1.202	0.938	1.110	0.942	1.088	0.942	0.967	0.947
	[2]	1.145	0.940	1.076	0.943	1.046	0.944	1.024	0.945	0.784	0.953	0.759	0.954
	[3]	1.163	0.940	1.241	0.937	1.114	0.942	1.081	0.943	0.984	0.946	0.887	0.950
(30,20)	[1]	1.066	0.943	0.923	0.948	0.866	0.950	0.753	0.955	0.742	0.955	0.538	0.962
	[2]	1.057	0.944	0.918	0.949	0.771	0.954	0.737	0.955	0.733	0.955	0.517	0.963
	[3]	1.093	0.942	1.008	0.945	0.954	0.947	0.801	0.953	0.762	0.954	0.553	0.962
(50,20)	[1]	1.008	0.945	0.850	0.951	0.739	0.955	0.720	0.956	0.644	0.958	0.505	0.964
	[2]	0.849	0.951	0.687	0.957	0.661	0.958	0.655	0.958	0.630	0.959	0.478	0.964
	[3]	0.877	0.950	0.820	0.952	0.681	0.957	0.659	0.958	0.638	0.959	0.496	0.964
(50,40)	[1]	0.837	0.952	0.620	0.959	0.616	0.960	0.613	0.960	0.572	0.961	0.402	0.967
	[2]	0.809	0.953	0.617	0.959	0.610	0.960	0.579	0.961	0.563	0.961	0.396	0.967
	[3]	0.849	0.951	0.635	0.959	0.629	0.959	0.623	0.959	0.618	0.959	0.404	0.967
(80,30)	[1]	0.743	0.955	0.574	0.961	0.557	0.962	0.545	0.962	0.537	0.962	0.387	0.968
	[2]	0.726	0.956	0.537	0.962	0.485	0.964	0.474	0.965	0.465	0.965	0.375	0.968
	[3]	0.732	0.955	0.537	0.962	0.497	0.964	0.495	0.964	0.494	0.964	0.385	0.968
(80,60)	[1]	0.631	0.959	0.516	0.963	0.477	0.965	0.448	0.966	0.321	0.970	0.275	0.972
	[2]	0.536	0.962	0.506	0.963	0.456	0.965	0.418	0.967	0.299	0.971	0.269	0.972
	[3]	0.716	0.956	0.522	0.963	0.479	0.964	0.467	0.965	0.451	0.965	0.372	0.968
Set 2 (for T = 0.5)													
(30,10)	[1]	1.919	0.927	1.886	0.928	1.357	0.943	1.203	0.947	0.985	0.953	0.944	0.954
	[2]	1.666	0.934	1.250	0.946	1.150	0.948	1.020	0.952	0.851	0.957	0.799	0.958
	[3]	2.240	0.918	1.923	0.927	1.486	0.939	1.298	0.944	1.120	0.949	1.044	0.951
(30,20)	[1]	1.491	0.939	1.212	0.947	1.011	0.952	0.955	0.954	0.838	0.957	0.778	0.959
	[2]	1.170	0.948	0.932	0.954	0.851	0.957	0.812	0.958	0.801	0.958	0.740	0.960
	[3]	1.221	0.946	1.002	0.952	0.953	0.954	0.915	0.955	0.813	0.958	0.759	0.959
(50,20)	[1]	0.854	0.957	0.806	0.958	0.771	0.959	0.765	0.959	0.739	0.960	0.692	0.961
	[2]	0.818	0.958	0.718	0.960	0.683	0.961	0.676	0.961	0.676	0.962	0.644	0.962
	[3]	0.894	0.955	0.812	0.958	0.782	0.959	0.776	0.959	0.740	0.960	0.722	0.960
(50,40)	[1]	0.783	0.959	0.673	0.962	0.666	0.962	0.663	0.962	0.618	0.963	0.583	0.964
	[2]	0.688	0.961	0.617	0.963	0.613	0.963	0.610	0.963	0.590	0.964	0.560	0.965
	[3]	0.742	0.960	0.673	0.962	0.640	0.963	0.618	0.963	0.606	0.963	0.569	0.964
(80,30)	[1]	0.599	0.964	0.580	0.964	0.572	0.964	0.567	0.965	0.537	0.965	0.526	0.966
	[2]	0.575	0.964	0.537	0.965	0.529	0.966	0.515	0.966	0.510	0.966	0.507	0.966
	[3]	0.621	0.963	0.602	0.964	0.599	0.964	0.588	0.964	0.556	0.965	0.530	0.966
(80,60)	[1]	0.543	0.965	0.514	0.966	0.512	0.966	0.509	0.966	0.506	0.966	0.500	0.966
	[2]	0.493	0.967	0.473	0.967	0.466	0.967	0.454	0.968	0.441	0.968	0.407	0.969
	[3]	0.511	0.966	0.506	0.966	0.477	0.967	0.463	0.967	0.462	0.967	0.445	0.968
Set 2 (for T = 1.5)													
(30,10)	[1]	1.981	0.925	1.588	0.936	1.040	0.951	1.020	0.952	0.999	0.953	0.891	0.956
	[2]	1.451	0.940	1.243	0.946	1.025	0.952	1.013	0.952	0.846	0.957	0.795	0.958
	[3]	2.147	0.921	1.719	0.932	1.369	0.942	1.117	0.949	1.097	0.950	0.990	0.953
(30,20)	[1]	1.353	0.943	1.186	0.947	1.003	0.952	0.933	0.954	0.836	0.957	0.774	0.959
	[2]	0.965	0.953	0.925	0.955	0.847	0.957	0.810	0.958	0.794	0.958	0.736	0.960
	[3]	1.111	0.949	0.996	0.953	0.931	0.954	0.913	0.955	0.810	0.958	0.756	0.959
(50,20)	[1]	0.810	0.958	0.802	0.958	0.765	0.959	0.760	0.959	0.733	0.960	0.689	0.961
	[2]	0.790	0.958	0.714	0.960	0.680	0.961	0.676	0.961	0.675	0.962	0.642	0.962
	[3]	0.829	0.957	0.810	0.958	0.778	0.959	0.775	0.959	0.736	0.960	0.719	0.960
(50,40)	[1]	0.758	0.959	0.667	0.962	0.663	0.962	0.660	0.962	0.616	0.963	0.581	0.964
	[2]	0.640	0.962	0.615	0.963	0.610	0.963	0.608	0.963	0.589	0.964	0.558	0.965
	[3]	0.720	0.960	0.667	0.962	0.639	0.963	0.616	0.963	0.604	0.963	0.567	0.965
(80,30)	[1]	0.576	0.964	0.579	0.964	0.572	0.964	0.567	0.965	0.535	0.965	0.524	0.966
	[2]	0.563	0.965	0.535	0.965	0.527	0.966	0.512	0.966	0.509	0.966	0.505	0.966
	[3]	0.606	0.963	0.600	0.964	0.597	0.964	0.585	0.964	0.552	0.965	0.526	0.966
(80,60)	[1]	0.527	0.966	0.512	0.966	0.510	0.966	0.509	0.966	0.504	0.966	0.500	0.966
	[2]	0.487	0.967	0.472	0.967	0.465	0.967	0.453	0.968	0.439	0.968	0.406	0.969
	[3]	0.509	0.966	0.504	0.966	0.476	0.967	0.463	0.967	0.462	0.967	0.443	0.968

Table S7. The AILs (1st col.) and CPs (2nd col.) of $R(t)$.

(n, k)		ACI-NA		ACI-NL		BCI [Prior A]		BCI [Prior B]		HPD [Prior A]		HPD [Prior B]	
Set 1 (for T = 0.5)													
(30,10)	[1]	0.171	0.928	0.102	0.953	0.081	0.960	0.076	0.962	0.070	0.964	0.049	0.971
	[2]	0.139	0.939	0.097	0.954	0.065	0.966	0.055	0.969	0.052	0.970	0.023	0.977
	[3]	0.165	0.930	0.099	0.954	0.074	0.962	0.061	0.967	0.056	0.969	0.034	0.972
(30,20)	[1]	0.096	0.954	0.069	0.964	0.057	0.968	0.033	0.977	0.030	0.978	0.013	0.983
	[2]	0.090	0.957	0.063	0.966	0.052	0.970	0.028	0.979	0.027	0.979	0.010	0.984
	[3]	0.107	0.951	0.070	0.964	0.063	0.966	0.044	0.973	0.042	0.974	0.017	0.980
(50,20)	[1]	0.072	0.963	0.063	0.966	0.051	0.970	0.027	0.979	0.024	0.980	0.009	0.985
	[2]	0.061	0.967	0.059	0.968	0.036	0.976	0.023	0.981	0.020	0.982	0.008	0.986
	[3]	0.071	0.964	0.059	0.968	0.038	0.975	0.025	0.980	0.022	0.981	0.009	0.986
(50,40)	[1]	0.048	0.972	0.045	0.973	0.028	0.979	0.017	0.982	0.015	0.983	0.007	0.986
	[2]	0.042	0.974	0.036	0.976	0.024	0.980	0.014	0.983	0.013	0.984	0.007	0.986
	[3]	0.056	0.969	0.051	0.971	0.032	0.977	0.020	0.982	0.018	0.982	0.008	0.986
(80,30)	[1]	0.035	0.976	0.032	0.977	0.022	0.981	0.015	0.983	0.012	0.984	0.006	0.986
	[2]	0.030	0.978	0.020	0.982	0.018	0.982	0.012	0.984	0.010	0.985	0.005	0.987
	[3]	0.033	0.977	0.031	0.978	0.020	0.982	0.015	0.984	0.011	0.985	0.006	0.987
(80,60)	[1]	0.021	0.981	0.017	0.983	0.014	0.984	0.010	0.985	0.007	0.986	0.005	0.987
	[2]	0.017	0.983	0.010	0.984	0.012	0.985	0.009	0.985	0.005	0.987	0.005	0.987
	[3]	0.025	0.980	0.020	0.982	0.015	0.983	0.012	0.985	0.009	0.985	0.005	0.987
Set 1 (for T = 1.5)													
(30,10)	[1]	0.162	0.928	0.095	0.953	0.076	0.961	0.069	0.962	0.063	0.964	0.043	0.972
	[2]	0.132	0.939	0.090	0.954	0.060	0.966	0.049	0.970	0.047	0.970	0.020	0.981
	[3]	0.157	0.930	0.092	0.954	0.069	0.963	0.054	0.967	0.050	0.969	0.030	0.977
(30,20)	[1]	0.092	0.954	0.064	0.964	0.053	0.969	0.030	0.977	0.027	0.978	0.012	0.984
	[2]	0.086	0.957	0.059	0.966	0.049	0.970	0.025	0.979	0.024	0.979	0.009	0.985
	[3]	0.101	0.951	0.065	0.964	0.059	0.967	0.040	0.973	0.038	0.975	0.015	0.983
(50,20)	[1]	0.069	0.963	0.059	0.966	0.048	0.971	0.024	0.980	0.022	0.980	0.008	0.986
	[2]	0.058	0.967	0.054	0.968	0.033	0.976	0.021	0.981	0.018	0.982	0.007	0.986
	[3]	0.067	0.964	0.055	0.968	0.035	0.975	0.023	0.980	0.020	0.982	0.007	0.986
(50,40)	[1]	0.045	0.972	0.042	0.973	0.026	0.979	0.016	0.982	0.014	0.983	0.006	0.986
	[2]	0.040	0.974	0.033	0.976	0.022	0.981	0.012	0.983	0.012	0.984	0.006	0.986
	[3]	0.054	0.969	0.047	0.971	0.030	0.978	0.018	0.982	0.016	0.983	0.007	0.986
(80,30)	[1]	0.033	0.976	0.029	0.977	0.021	0.981	0.014	0.984	0.011	0.985	0.005	0.987
	[2]	0.029	0.978	0.018	0.982	0.017	0.982	0.011	0.985	0.009	0.985	0.005	0.987
	[3]	0.031	0.977	0.029	0.978	0.019	0.982	0.013	0.984	0.010	0.985	0.005	0.987
(80,60)	[1]	0.020	0.981	0.016	0.983	0.013	0.984	0.009	0.985	0.007	0.986	0.005	0.988
	[2]	0.016	0.983	0.010	0.985	0.011	0.985	0.008	0.986	0.005	0.987	0.004	0.989
	[3]	0.024	0.980	0.018	0.982	0.014	0.984	0.010	0.985	0.008	0.985	0.004	0.988
Set 2 (for T = 0.5)													
(30,10)	[1]	0.185	0.929	0.174	0.932	0.073	0.960	0.069	0.965	0.040	0.974	0.039	0.975
	[2]	0.147	0.941	0.130	0.946	0.063	0.964	0.062	0.968	0.039	0.975	0.037	0.975
	[3]	0.196	0.925	0.189	0.927	0.086	0.955	0.083	0.961	0.062	0.967	0.053	0.970
(30,20)	[1]	0.130	0.946	0.129	0.946	0.062	0.967	0.056	0.969	0.037	0.975	0.029	0.978
	[2]	0.124	0.948	0.117	0.950	0.049	0.969	0.035	0.976	0.034	0.976	0.019	0.981
	[3]	0.125	0.947	0.118	0.948	0.056	0.967	0.037	0.975	0.035	0.976	0.021	0.980
(50,20)	[1]	0.104	0.954	0.088	0.959	0.031	0.973	0.030	0.978	0.023	0.980	0.013	0.983
	[2]	0.088	0.959	0.060	0.968	0.029	0.977	0.027	0.979	0.022	0.980	0.011	0.984
	[3]	0.105	0.954	0.098	0.956	0.045	0.972	0.032	0.977	0.028	0.978	0.015	0.982
(50,40)	[1]	0.078	0.962	0.060	0.968	0.022	0.978	0.015	0.982	0.013	0.984	0.009	0.984
	[2]	0.077	0.963	0.046	0.973	0.018	0.980	0.013	0.983	0.010	0.984	0.008	0.985
	[3]	0.079	0.962	0.055	0.970	0.021	0.980	0.014	0.983	0.012	0.984	0.008	0.985
(80,30)	[1]	0.043	0.974	0.024	0.981	0.015	0.982	0.011	0.984	0.008	0.985	0.006	0.985
	[2]	0.024	0.979	0.021	0.981	0.012	0.982	0.010	0.984	0.007	0.985	0.006	0.985
	[3]	0.045	0.973	0.030	0.978	0.017	0.981	0.012	0.983	0.009	0.984	0.007	0.985
(80,60)	[1]	0.024	0.980	0.017	0.982	0.011	0.983	0.010	0.984	0.007	0.985	0.005	0.985
	[2]	0.021	0.980	0.012	0.983	0.103	0.984	0.006	0.985	0.004	0.986	0.004	0.986
	[3]	0.023	0.980	0.015	0.982	0.009	0.984	0.007	0.985	0.006	0.985	0.005	0.985
Set 2 (for T = 1.5)													
(30,10)	[1]	0.176	0.929	0.162	0.933	0.068	0.965	0.062	0.966	0.036	0.975	0.034	0.975
	[2]	0.139	0.941	0.121	0.946	0.058	0.967	0.056	0.968	0.035	0.975	0.032	0.976
	[3]	0.187	0.925	0.176	0.928	0.080	0.960	0.075	0.961	0.056	0.968	0.046	0.971
(30,20)	[1]	0.123	0.946	0.120	0.946	0.058	0.968	0.051	0.970	0.034	0.975	0.026	0.978
	[2]	0.118	0.948	0.109	0.950	0.045	0.972	0.031	0.976	0.031	0.977	0.017	0.981
	[3]	0.119	0.948	0.110	0.950	0.052	0.970	0.033	0.976	0.032	0.976	0.019	0.980
(50,20)	[1]	0.098	0.954	0.082	0.959	0.029	0.978	0.027	0.978	0.021	0.980	0.011	0.983
	[2]	0.084	0.959	0.056	0.968	0.027	0.978	0.024	0.979	0.020	0.980	0.010	0.984
	[3]	0.100	0.954	0.091	0.956	0.042	0.973	0.029	0.977	0.025	0.978	0.013	0.983
(50,40)	[1]	0.074	0.962	0.056	0.968	0.021	0.980	0.014	0.983	0.012	0.984	0.008	0.984
	[2]	0.073	0.968	0.042	0.973	0.017	0.982	0.012	0.983	0.009	0.984	0.007	0.985
	[3]	0.075	0.967	0.051	0.970	0.020	0.981	0.012	0.983	0.011	0.984	0.007	0.985
(80,30)	[1]	0.041	0.974	0.022	0.981	0.014	0.982	0.010	0.984	0.007	0.985	0.006	0.985
	[2]	0.023	0.979	0.019	0.981	0.012	0.983	0.009	0.984	0.006	0.985	0.005	0.985
	[3]	0.042	0.973	0.028	0.978	0.016	0.982	0.010	0.984	0.008	0.984	0.006	0.985
(80,60)	[1]	0.023	0.980	0.016	0.982	0.010	0.983	0.009	0.984	0.006	0.985	0.005	0.985
	[2]	0.020	0.981	0.012	0.983	0.096	0.985	0.005	0.985	0.003	0.986	0.003	0.986
	[3]	0.022	0.980	0.014	0.983	0.009	0.985	0.006	0.985	0.006	0.985	0.004	0.986

Table S8. The AILs (1st col.) and CPs (2nd col.) of $h(t)$.

(n,k)		ACI-NA		ACI-NL		BCI [Prior A]		BCI [Prior B]		HPD [Prior A]		HPD [Prior B]	
Set 1 (for T = 0.5)													
(30,10)	[1]	1.961	0.917	1.348	0.938	1.144	0.945	0.987	0.950	0.904	0.953	0.414	0.970
	[2]	2.071	0.913	1.586	0.930	1.341	0.938	1.088	0.947	0.979	0.951	0.601	0.964
	[3]	2.190	0.909	1.650	0.928	1.445	0.935	1.349	0.938	1.246	0.941	0.857	0.955
(30,20)	[1]	1.473	0.934	1.140	0.945	0.932	0.952	0.524	0.966	0.470	0.968	0.188	0.978
	[2]	1.813	0.922	1.190	0.943	1.118	0.946	0.802	0.957	0.737	0.959	0.303	0.974
	[3]	1.599	0.929	1.172	0.944	1.010	0.950	0.576	0.964	0.566	0.965	0.239	0.976
(50,20)	[1]	1.069	0.947	1.014	0.949	0.680	0.961	0.367	0.972	0.331	0.973	0.154	0.979
	[2]	1.310	0.939	1.023	0.949	0.708	0.960	0.451	0.969	0.367	0.972	0.158	0.979
	[3]	1.393	0.936	1.130	0.945	0.910	0.953	0.498	0.967	0.428	0.970	0.159	0.979
(50,40)	[1]	0.695	0.960	0.667	0.961	0.425	0.970	0.249	0.976	0.233	0.976	0.127	0.980
	[2]	1.007	0.950	0.858	0.955	0.562	0.965	0.348	0.972	0.317	0.973	0.146	0.979
	[3]	0.779	0.957	0.762	0.958	0.472	0.968	0.310	0.974	0.272	0.975	0.127	0.980
(80,30)	[1]	0.518	0.966	0.398	0.971	0.318	0.973	0.212	0.977	0.176	0.978	0.102	0.981
	[2]	0.595	0.964	0.541	0.966	0.349	0.972	0.239	0.976	0.188	0.978	0.105	0.981
	[3]	0.599	0.964	0.565	0.965	0.386	0.971	0.239	0.976	0.219	0.977	0.122	0.980
(80,60)	[1]	0.321	0.973	0.196	0.977	0.184	0.978	0.127	0.980	0.093	0.981	0.073	0.982
	[2]	0.486	0.968	0.362	0.972	0.268	0.975	0.212	0.977	0.174	0.978	0.099	0.981
	[3]	0.396	0.971	0.305	0.974	0.245	0.976	0.185	0.978	0.136	0.980	0.093	0.981
Set 1 (for T = 1.5)													
(30,10)	[1]	1.760	0.924	1.266	0.941	1.114	0.946	0.958	0.951	0.897	0.953	0.396	0.971
	[2]	1.818	0.922	1.444	0.935	1.299	0.940	1.072	0.947	0.967	0.951	0.581	0.964
	[3]	1.976	0.916	1.471	0.934	1.403	0.936	1.310	0.939	1.225	0.942	0.835	0.956
(30,20)	[1]	1.434	0.935	1.069	0.947	0.919	0.953	0.511	0.967	0.463	0.968	0.181	0.978
	[2]	1.739	0.924	1.126	0.946	1.103	0.946	0.779	0.957	0.701	0.960	0.295	0.974
	[3]	1.558	0.931	1.092	0.947	1.004	0.950	0.575	0.964	0.561	0.965	0.232	0.976
(50,20)	[1]	1.016	0.949	0.950	0.952	0.662	0.961	0.363	0.972	0.325	0.973	0.151	0.979
	[2]	1.259	0.941	0.974	0.951	0.694	0.960	0.431	0.969	0.351	0.972	0.153	0.979
	[3]	1.306	0.939	1.055	0.948	0.904	0.953	0.475	0.968	0.409	0.970	0.154	0.979
(50,40)	[1]	0.677	0.961	0.626	0.963	0.410	0.970	0.242	0.976	0.233	0.976	0.124	0.980
	[2]	0.947	0.952	0.827	0.956	0.542	0.966	0.336	0.973	0.304	0.974	0.141	0.979
	[3]	0.766	0.958	0.733	0.959	0.467	0.968	0.297	0.974	0.267	0.975	0.124	0.980
(80,30)	[1]	0.510	0.967	0.390	0.971	0.309	0.974	0.201	0.977	0.171	0.978	0.101	0.981
	[2]	0.578	0.964	0.525	0.966	0.344	0.972	0.230	0.976	0.184	0.978	0.104	0.981
	[3]	0.588	0.964	0.554	0.965	0.375	0.971	0.230	0.976	0.212	0.977	0.118	0.980
(80,60)	[1]	0.299	0.974	0.185	0.978	0.176	0.978	0.122	0.980	0.091	0.981	0.064	0.982
	[2]	0.444	0.969	0.350	0.972	0.262	0.975	0.201	0.977	0.169	0.978	0.096	0.981
	[3]	0.370	0.972	0.299	0.974	0.236	0.976	0.176	0.978	0.132	0.980	0.091	0.981
Set 2 (for T = 0.5)													
(30,10)	[1]	2.291	0.915	1.798	0.929	1.289	0.944	1.153	0.948	0.809	0.958	0.725	0.960
	[2]	2.368	0.913	1.866	0.928	1.419	0.940	1.318	0.943	0.841	0.957	0.753	0.960
	[3]	2.507	0.909	1.961	0.925	1.635	0.934	1.579	0.936	1.160	0.948	0.975	0.953
(30,20)	[1]	2.025	0.923	1.655	0.934	0.899	0.955	0.658	0.962	0.634	0.963	0.375	0.971
	[2]	2.207	0.918	1.722	0.932	1.151	0.948	1.029	0.952	0.714	0.961	0.581	0.965
	[3]	2.135	0.920	1.692	0.933	1.015	0.952	0.701	0.961	0.681	0.962	0.410	0.970
(50,20)	[1]	1.740	0.931	1.306	0.944	0.614	0.964	0.503	0.967	0.462	0.968	0.231	0.975
	[2]	1.801	0.929	1.533	0.937	0.637	0.963	0.590	0.964	0.481	0.968	0.265	0.974
	[3]	1.932	0.926	1.581	0.936	0.853	0.957	0.615	0.964	0.555	0.965	0.309	0.972
(50,40)	[1]	1.266	0.945	0.843	0.957	0.373	0.971	0.257	0.974	0.206	0.975	0.157	0.977
	[2]	1.479	0.939	1.244	0.945	0.437	0.969	0.307	0.973	0.220	0.975	0.179	0.976
	[3]	1.374	0.942	1.059	0.951	0.434	0.969	0.273	0.974	0.209	0.975	0.166	0.977
(80,30)	[1]	0.491	0.967	0.405	0.970	0.259	0.974	0.211	0.975	0.152	0.977	0.123	0.978
	[2]	0.906	0.955	0.410	0.970	0.332	0.972	0.216	0.975	0.161	0.977	0.135	0.978
	[3]	0.925	0.955	0.594	0.964	0.332	0.972	0.232	0.975	0.206	0.975	0.147	0.977
(80,60)	[1]	0.423	0.969	0.248	0.974	0.140	0.977	0.132	0.978	0.089	0.979	0.084	0.979
	[2]	0.487	0.967	0.356	0.971	0.259	0.974	0.207	0.975	0.152	0.977	0.114	0.978
	[3]	0.442	0.969	0.285	0.973	0.148	0.977	0.144	0.977	0.139	0.977	0.112	0.978
Set 2 (for T = 1.5)													
(30,10)	[1]	2.245	0.917	1.726	0.932	1.250	0.945	1.144	0.948	0.784	0.959	0.698	0.961
	[2]	2.294	0.915	1.727	0.932	1.388	0.941	1.282	0.944	0.817	0.958	0.735	0.960
	[3]	2.347	0.914	1.796	0.930	1.603	0.935	1.542	0.937	1.147	0.948	0.964	0.954
(30,20)	[1]	1.942	0.925	1.527	0.937	0.891	0.956	0.642	0.963	0.626	0.963	0.366	0.971
	[2]	2.187	0.918	1.696	0.932	1.135	0.949	1.014	0.952	0.705	0.961	0.559	0.965
	[3]	1.973	0.924	1.615	0.935	1.007	0.952	0.697	0.961	0.674	0.962	0.403	0.970
(50,20)	[1]	1.570	0.936	1.215	0.946	0.596	0.964	0.488	0.967	0.453	0.968	0.223	0.975
	[2]	1.722	0.932	1.449	0.940	0.623	0.963	0.569	0.965	0.472	0.968	0.256	0.974
	[3]	1.790	0.930	1.490	0.938	0.839	0.957	0.591	0.964	0.543	0.966	0.300	0.973
(50,40)	[1]	1.143	0.948	0.792	0.959	0.347	0.971	0.248	0.974	0.201	0.976	0.152	0.977
	[2]	1.383	0.941	1.187	0.947	0.420	0.969	0.293	0.973	0.213	0.975	0.173	0.976
	[3]	1.286	0.944	0.992	0.953	0.414	0.969	0.255	0.974	0.203	0.976	0.160	0.977
(80,30)	[1]	0.470	0.968	0.396	0.970	0.243	0.974	0.200	0.976	0.146	0.977	0.119	0.978
	[2]	0.815	0.958	0.398	0.970	0.322	0.972	0.209	0.975	0.154	0.977	0.129	0.978
	[3]	0.836	0.957	0.550	0.966	0.322	0.972	0.219	0.975	0.201	0.976	0.144	0.977
(80,60)	[1]	0.408	0.970	0.237	0.975	0.135	0.978	0.130	0.978	0.088	0.979	0.083	0.979
	[2]	0.440	0.969	0.333	0.972	0.243	0.974	0.194	0.976	0.146	0.977	0.110	0.978
	[3]	0.423	0.969	0.273	0.974	0.146	0.977	0.140	0.977	0.135	0.978	0.108	0.978

Appendix 2

This appendix includes lists of all abbreviations and symbols with their meanings in separate tables for clarification.

Table 22. List of abbreviations.

Abbreviation	Full Term
ACI	Asymptotic Confidence Interval
ACI-NA	ACI based on Normal Approximation
ACI-NL	ACI based on Log-Transformation
AI	Akaike Information
AIL	Average Interval Length
ARAB	Absolute Relative Average Bias
BCI	Bootstrap Confidence Interval
BI	Bayesian Information
CAI	Consistent Akaike Information
CDF	Cumulative Distribution Function
CI	Confidence Interval
CP	Coverage Probability
FIM	Fisher Information Matrix
FR	Failure Rate
HPD	Highest Posterior Density
HRF	Hazard Rate Function
HQI	Hannan-Quinn Information
IFR	Increasing Failure Rate
KS	Kolmogorov–Smirnov
LF	Likelihood Function
ML	Maximum Likelihood
MLE	Maximum Likelihood Estimator
MCMC	Markov Chain Monte Carlo
NA	Normal Approximation
NL	Normal Log-Transformed
NLL	Negative Log-Likelihood
PDF	Probability Density Function
P-P	Probability–Probability
Q-Q	Quantile–Quantile
RMSE	Root Mean Squared Error
T2-PC	Progressive Type-II Censoring
T2A-PC	Adaptive Progressive Type-II Censoring
VCM	Variance–Covariance Matrix
VFW	Very Flexible Weibull

Table 23. List of symbols.

Symbol	Description
(γ, δ)	Parameters of VFW distribution
$C(\theta)$	Normalizing constant of the distribution
$g(x)$	Probability density function
$G(x)$	Cumulative distribution function
$h(x)$	Hazard rate function
$\mathbf{F}(\theta)$	Fisher information matrix
k	Number of observed failures
$L(\theta)$	Likelihood function
$\ell(\theta)$	Log-likelihood function
n	Complete sample size
R_i	Number of units removed at the i-th failure time
S	Number of progressive censoring stages
T	Threshold
$R(x)$	Reliability function
x_i	Observed failure time at the i-th stage
$\hat{\theta}$	Maximum likelihood estimator of θ
$\hat{\varepsilon}_{11}$	Variance of $\hat{\gamma}$
$\hat{\varepsilon}_{22}$	Variance of $\hat{\delta}$
φ	Significance level
d	Total number of failure times up to T
$\mathbf{F}^{-1}(\cdot)$	Variance–covariance matrix
θ	Vector of model parameters